Comparative Analysis of MODIS, MISR and AERONET Climatology over the Middle East and North Africa

Ashraf Farahat

Department of Physics, King Fahd University of Petroleum and Minerals, Dhahran 31261, Saudi Arabia;
E-Mails: farahata@kfupm.edu.sa

*Author to whom correspondence should be addressed; E-Mail: farahata@kfupm.edu.sa.
Tel: (321) 541-7088

Abstract:

Comparative analysis of MISR MODIS, and AERONET AOD products is performed over seven AERONET stations located in the Middle East and North Africa for the period of 2000 – 2015. Sites are categorized into dust, biomass burning and mixed. MISR and MODIS AOD agree during high dust seasons but MODIS tends to underestimate AOD during low dust seasons. Over dust dominated sites, MODIS/Terra AOD indicate a negative trend over the time series, while MODIS/Aqua, MISR, and AERONET depict a positive trend. A deviation between MODIS/Aqua and MODIS/Terra was observed regardless of the geographic location and data sampling. The performance of MODIS is similar over the entire region with ~64 percent of AOD within the $\Delta\tau = \pm 0.05 \pm 0.15\tau_{AERO}$ confidence range. MISR AOD retrievals fall within 84 percent of the same confidence range for all sites examined here. Both MISR and MODIS capture aerosol climatology; however few cases were observed where one of the two sensors better captures the climatology over a certain location or AOD range than the other sensor. AERONET Level 2.0 Version 3, MODIS Collection 6.1, and MISR V23 data have been used in analyzing the results presented in this study

Keywords: AOD; Remote Sensing; North Africa; Middle East; Validation

1. Introduction

The Middle East and North Africa host the largest dust source in the world, the Sahara Desert in North Africa that may be responsible for up to 18 percent of global dust emission (Todd et al., 2007, Bou Karam et al. 2010, Schepanski et al. 2016). The vast 650,000 km^2 Rub' al Khali (Empty Quarter) sand desert is a major source of frequent dust outbreaks and severe dust storms that has major effect on human activity in the Arabian Peninsula (Böer, 1997, Elagib and Addin 1997, Farahat et al., 2015).

Air quality over the Arabian Peninsula has received significant attention during the past 15 years due to unprecedented overall economic growth, and a booming oil and gas industry, however, air pollution studies are still far from complete. Frequently blowing dust storms play a significant role in pollutant transport over the Arabian Peninsula; and major environmental pollution events such as burning of Kuwait oil fields during the 1991, Gulf War resulted in a large environmental impact on the Arabian Gulf Area (Sadiq and McCain, 1993, and Farahat 2016).

Aerosol optical depth, AOD, (also called aerosol optical thickness, AOT) as a parameter indicates the extinction of a beam of radiation as it passes through a layer of atmosphere that contains aerosols. Both satellites and ground-based instruments can be used to measure AOD in the atmosphere, but within the same temporal coordinates and geographic location different instruments could generate different retrievals (Kahn et al., 2007, Kokhanovsky et al., 2007, Liu et al., 2008 and Mishchenko et al., 2009).

Since the turn of the 21st century, an upward trend of remotely sensed and ground-based AOD and air pollutants was observed over the Middle East and North Africa (El-Askary 2009, Ansmann et al. 2011, Yu et al. 2013, Chin et al. 2014, Yu et al. 2015, Farahat et al. 2016, Solomos et al. 2017). This positive trend is attributed to the increase in the Middle Eastern dust activity (Hsu et al., 2012) due to changes in wind speed and soil moisture (Ginoux et al. 2001 and Kim et al. 2013). Yu et al., (2015) concluded that the persistent La

Niña conditions (Hoell et al., 2013) have caused increment in Saudi Arabian dust activity during 2008 – 2012. Energy subsidies also encourages energy overconsumption in the Middle East and North Africa with little incentive to adopt cleaner technology. Lack of applying strict environmental regulations have permitted exacerbated urban air pollution.

During the last two decades, a large number of satellites, ground stations and computational models contributed to build global and regional maps for the temporal and spatial aerosol distributions. While, ground-based stations and field measurements can identify aerosols properties over specific geographic locations, the spare and non-continues data from ground-based sensors scattered over the Middle East and North Africa is not sufficient to provide information on spatial and temporal trends of particulate pollution. On the other hand, satellites imagery could provide a significant source of data mapping over larger areas.

For its wide spatial and temporal data availability space-born sensors are important sources to understand aerosols characteristics and transport, however low sensitivity to particle type under some physical conditions, high surface reflectivity, persistent cloud, and generally low aerosol optical depth could limit satellite data application in characterizing properties of airborne particles, especially in the Middle East.

In order to evaluate the efficiency of space-borne sensors in representing ground observations recorded by AERONET stations we have performed detailed statistical inter-comparison analysis between satellite AOD products and AERONET for seven stations in the Middle East and North Africa representative for dust, biomass burning, and mixed aerosol conditions (Dubovik et al., (2000, 2002, 2006), Holben et al. (2001), Derimian et al., (2006), Basart et al. (2009), Eck el. (2010), Marey et al., 2010, Abdi et al., (2012)). Previously we analysed these seven AERONET stations to understand particles categorization and absorption properties (Farahat et al. 2016), and the current study extends the analysis to the satellite datasets.

In the first part of this article, we validated MISR and MODIS retrievals against collocated AERONET observations. We also assessed the consistency in aerosol trends between space-borne sensors and ground-based data.

In the second part, we evaluated representativeness of satellite-derived aerosol climatology over the study region from the long-term AERONET data for MISR and MODIS AOD products. It is especially relevant for the MISR instrument, as its sampling is limited by once per week observations of the same region from the two overlapping paths. MODIS provides nearly daily observations to the same geographic location; however, the quality of the product diminishes over the bright targets potentially affecting MODIS-derived aerosol climatology. The collocated MISR, MODIS and AERONET data were obtained at the MAPSS website (http://giovanni.gsfc.nasa.gov/mapss.html).

2. Materials and Methods

2.1 MISR

The Multi-angle Imaging SpectroRadimeter (MISR) instrument to measure tropospheric aerosol characteristics through the acquisition of global multi-angle imagery on the daylight side of Earth. MISR applies nine Charge Coupled Devices (CCDs), each with 4 independent line arrays positioned at nine view angles spread out at nadir, 26.1^{o}, 45.6^{o}, 60.0^{o}, and 70.5^{o}. In each of the nine MISR cameras, images are obtained from reflected and scattered sunlight in 4 bands blue, green, red, and near-infrared with a centre wavelength value of 446, 558, 672, and 867 nm respectively. The combination of viewing cameras and spectral wavelengths enables MISR to retrieve aerosols AOD over high reflection surfaces like deserts.

In this study, we use Level 2 (ver. 0023) AOD at 558 nm (green band) measured by MISR instrument with a 17.6 km resolution aboard the Terra satellite. MISR Level 2 aerosol retrievals use only data that pass angle-to-angle smoothness and spatial correlation tests

(Martonchik et al. 2002), as well as stereoscopically derived cloud masks and adaptive cloud-screening brightness thresholds (Zhao and Di Girolamo, 2004).

2.2 MODIS

The Moderate Resolution Imaging Spectroradiometer (MODIS) is a payload instrument on board the Terra and Aqua satellites. Terra and Aqua orbit around the Earth from North to South and South to North across the equator during the morning and afternoon respectively (Kaufman et al., 1997). Terra MODIS and Aqua MODIS provides nearly daily coverage of the Earth's surface and atmosphere in 36 wavelength bands, ranging from 0.412 to 41.2 µm, with spatial resolutions of 250 m (bands 1-2), 500 m (bands 3-7), 1000 m (bands 8-36). Located near-polar orbit (705 km), MODIS has swath dimensions of 2330 km × 10 km and a scan rate of 20.3 rpm. With its high radiometric sensitivity and swath resolution MODIS retrievals provide information about aerosols optical and physical characteristics. MODIS uses 14 spectral band radiance values to evaluate atmospheric contamination and determine whether scenes are affected by cloud shadow (Ackerman et al., 1998).

The Deep Blue (DB) is a NASA developed algorithm to calculate AOD over land using MODIS data. By measuring contrast between aerosols and surface features, DB retrieves AOD. Over bright land, Deep Blue uses (0.412, 0.470/0.479 µm) for AOD retrievals. Over water, the DB algorithm is not used, but the Dark Target (DT) algorithm is used instead.

The MODIS DT algorithm is designed for aerosol retrieval from MODIS observations, over dark land surfaces (low values of surface reflectance) (e.g., dark soil and vegetated regions) in parts of the visible (VIS, 0.47 and 0.65 µm) and shortwave infrared (SWIR, 2.1 µm) spectrum (Kaufman et al., 1997). Level 2 – Collection 6 (C006) of the algorithm are used to retrieve MODIS aerosols' time series data. Levy *et al.* (2010) reported that the dark-target algorithm AOD at 550 nm measurement for Collection 5 (C005) includes uncertainty of $\pm (0.05\tau+0.03)$ and $\pm (0.15\tau+0.05)$ over ocean and land, respectively. This uncertainty is caused by uncertainties in computing cloud masking, surface reflectance, aerosol model type (e.g., single scattering albedo), pixels selections and instrument calibration.

Both DB and DT algorithms have been used in this study. DB data were used over land, while DT retrievals were used over water. For regions like Bahrain where large water body surrounds land, a combined DB and DT algorithm for land and ocean has been used. This is because the MODIS matched ground-based AERONET station in Bahrain (described in section 2.3 and Table 1) is located less than 2 km from the coastline. This makes MODIS combine retrievals for both land and water over this region. Data are available at https://giovanni.gsfc.nasa.gov/giovanni.

2.3 AERONET

The Aerosol Robotic Network (AERONET) (Holben et al., 1998 and Holben et al., 2001) is a ground-based remote sensing aerosols network that provides a long-term data related to aerosol optical, microphysical and radiative properties. With over 700 global stations, the AERONET data is widely used in validating satellite retrievals (Chu et al., 1998 and Higurashi et al., 2000).

The sun photometers used by AERONET measure spectral direct-beam solar radiation, as well as directional diffuse radiation in the solar almucantar. The former are used to determine columnar spectral AOD and water vapour, provided at a temporal resolution of approximately 10–15 min (Sayer et al. 2014). AERONET direct-sun AOD has a typical uncertainty of 0.01–0.02 (Holben et al., 1998) and is provided at multiple wavelengths at 340, 380, 440, 500, 675, 950, and 1020 nm.

Seven AERONET sites were selected for satellite validation in this study (Table 1.). The sites were selected based on their geographic locations to represent aerosols characteristics over North Africa and the Middle East (Farahat et al., 2016). A record of long-term data collection was another factor in the selection process.

Data Matching Approach

Multi-sensors data matching requires using only compatible data to eliminate uncertainties associated with cloud shadow and spatial and temporal retrievals produced by different instruments (Liu and Mishchenko (2008) and Mishchenko et al., 2009).

The comparison of MISR and MODIS products against AERONET is performed to evaluate satellites' retrieval over individual North Africa and Middle East sites (see Table 1). There is only a small number of AERONET measurements that are perfectly collocated with MODIS and MISR. One way to work with this lack of compatibility problem is to compare satellites measurements nearby a certain AERONET site and comparing AERONET measurements nearly synchronized with the satellite overpass time (Sioris et al. 2017). Another reasonable strategy is to average all satellite measurements with a certain distance of an AERONET location and average all AERONET measurements within a certain time range (Mishchenko et al., 2010). The results presented in this paper are based on the second approach as it compares average spatial satellite measurements with average temporal AERONET measurements. We implemented the Basart et al., (2009) approach in using a spatial and temporal threshold of 50 km and 30 min for MISR, MODIS, and AERONET data matching.

We use the Giovanni Multi-sensor Aerosol Products Sampling System MAPSS (http://giovanni.gsfc.nasa.gov/aerostat/) for the data inter-comparison as aerosols products are averaged from measurements that are within a radius of ~ 27.5 km from the AERONET station and within 30 min of each satellite flyover over this location. These data are represented in the article by MISR / MODIS "matched AERONET data".

"All data" represents AOD products at the selected station. AERONET station 'all data' are obtained through AEROSOL ROBOTIC NETWORK (AERONET) website (https://aeronet.gsfc.nasa.gov/). Daily AOD data with level 2.0 quality was used in the analysis (Smirnov et al., 2000) . Level 2.0 AOD retrievals are accurate up to 0.02 for mid-visible wavelengths.

MISR 'all data' is available through MISR website (https://www misr.jpl.nasa.gov).

3. Statistics

We have used two statistical parameters to compare data retrievals from space-borne and ground based sensors including:

(1) Correlation coefficient (R),

The correlation coefficient is a parameter to measure data dependence. If the value of R is close to zero, it indicates weak data agreement. And values close to 1 or -1 indicate that data retrievals are positively or negatively linearly related (Cheng et al., 2012).

(2) Good Fraction (G- fraction).

The G- fraction indicator uses a data confidence range defined by MISR and MODIS (Bruegge et al., 1998 and Remer et al., 2005) over the land and ocean that combines absolute and relative criterion and weights data equally such that small abnormalities will not affect the inter-comparison statistics (Kahn et al., 2009). In this study, we use MODIS confidence range which defines data retrieval as "good" if the difference between MODIS and AERONET is less than

$$\Delta\tau = \pm 0.03 \pm 0.05\tau_{AER}, \quad \text{Over ocean,} \qquad (1)$$

$$\Delta\tau = \pm 0.05 \pm 0.15\tau_{AER}, \quad \text{Over land.} \qquad (2)$$

where τ_{AER} is the optical depth retrieved using AERONET stations. The G-fraction is the percentage of MODIS data retrievals that satisfies (Equations (1) and (2)) over ocean and land respectively. Optical depth threshold over land (Equation (1)) is higher than over ocean (Equation (2)) due to harder data retrievals and high data instability over land.

An advantage of using data confidence range is excluding small fraction data outliers from producing inexplicably large influence on comparison statistics by weighting all events equally.

4. Results and discussion

4.1 Validating MISR and MODIS AOD retrievals against AERONET observations over the Middle East and North Africa

Illustrated in Figures 2, 3 and Tables 2, 3 is a regression analysis of MISR and MODIS Terra AOD products against AERONET AOD over the seven AERONET sites, shown in Table1, from 2000 – 2015.

The correlation coefficient between MISR and AERONET AOD at region 1 is equal to or above 0.85 except in Bahrain during DJF and JJA (Figure (2) and Table 2), which could be attributed to lack of data and the impact of water surface reflectivity over Bahrain. Similar correlation coefficient values were found in region 2 where MISR-AERONET AOD shows smaller deviations from the MODIS data (Figures (2, 3) and Table 3). In general, MODIS-AERONET AOD correlation coefficient is lower than those of MISR at all sites, except Mezaira, where MISR and MODIS matched AERONET AOD correlation almost match. The lowest MODIS-AERONET AOD correlation coefficient was found over Cairo but could be attributed to the lack of data availability at this location (Figs 3e-h). Low values of MODIS-AERONET correlation coefficient is also found over Saada, Taman, and Sedee Boker sites.

Over all AERONET stations, the number of MODIS AERONET matched AOD are 4 to 8 times those of MISR which is expected from the MISR's sampling.

Comparisons show that the difference between MISR and MODIS retrievals at the selected AERONET sites could be significant as expected from the MODIS DT algorithm performance over bright land surfaces Kokhanovsky et al. (2007).

High AOD values over regions 1 and 2 measured by both AERONET and satellites' sensors indicate higher dust activities that peaks during May – Aug during dust storms season. Higher AOD values recorded during SON over Cairo station could be caused by seasonal rice straw burning by farmers in Cairo, an environmental phenomena known as Cairo Black cloud (Marey et al. 2010). As shown in (Figure (3)), the daily variability in MODIS measurements is larger than that of MISR in all the three regions. In general, MODIS tends to underestimate the AOD values on low dust seasons (Figures (2, 3) and Tables 2, 3).

The MODIS underestimated AOD values are more noticeable over Bahrain. This could be attributed to large water body surrounding Bahrain, which should affect surface reflectivity. Moreover, water in the Arabian Gulf has been polluted in recent years (Afnan 2013), leading to possible changes in watercolour and uncertainties in calculating surface reflectivity. The patchy land surface or pixel grid contaminated by water body is the dominant error sources for MODIS aerosol inversion over the land areas (He et al. 2010).

Compared to MODIS, MISR's outperform in retrieving AOD over region 1 including vast highly reflecting desert areas can be attributed to its multispectral and multi-angular coverage, which make MISR provide better viewing over a variety of landscapes. Meanwhile, MISR retrieval also takes into consideration aerosols' particles nonsphericity, which could have significant effect on its AOD retrievals (von Hoyningen-Huen and Posse 1997). MISR's retrieval did not perform well over Cairo site due to lack of matched points in most of the seasons (15 in DJF, 39 in MAM, 61 in JJA, and 23 in SON during 2000 - 2015).

4.2 Trends of AOD MISR, MODIS, and AERONET retrievals over the Middle East and North Africa

Figure 4 shows time series of monthly mean AOD derived from MODIS/Aqua, MODIS/Terra, MISR and AERONET over a) dust b) biomass and c) mixed dominated aerosol regions. The satellite AOD trends are calculated from the data collocated with AERONET observations.

MODIS/ Aqua and MISR AOD at Solar Village have positive trends, while MODIS/ Terra AOD have negative trends along time series (Fig. 4a). MODIS-Aqua AOD differ from those of MODIS-Terra. Discrepancy between Aqua and Terra retrievals could be related to instrument calibration, or the difference in aerosol and cloud conditions from the morning to the afternoon. Both MODIS Aqua and Terra are underestimating AOD at Solar Village.

MISR AOD trend shows a better agreement with Solar Village AERONET AOD as compared to MODIS.

Both MODIS/Aqua and MODIS/Terra AOD show a stable trend over time at Mezaria site (not shown in the figure) with a correlation coefficient of 0.11 and 0.04 respectively. MODIS/Aqua AOD over Bahrain (not shown in the figure) show, less time trend stability compared to those at Solar Village with a correlation coefficient 0.63. MODIS/Aqua, MODIS/Terra, and MISR AOD depicts a positive trend over Cairo (Fig. 4b). Taman site (Fig. 4c): MODIS/Aqua, MODIS/ Terra, MISR AOD agrees with Taman AERONET on a positive trend indicating data stability over this site.

Long-range (2000 – 2015) tendency indicates that contradictory AOD trend of Terra and Aqua is site-dependent and does not necessarily apply everywhere.

AOD difference between Terra and Aqua could be used as another indicator of the long-term satellites performance. AOD difference (Terra AOD minus Aqua AOD) varies from -0.01 to 0.19, -0.10 to 0.18 over Solar Village and Taman respectively (Fig. 5). Over the Solar

Village, Terra overestimates AOD during 2002-2004 and underestimates the AOD after 2005. Taman shows similar trend, however over/underestimation amount is not unique for all sites. This is an indication that Aqua and Terra retrievals disagreement takes place regardless of the region but site sampling has significant effect on the amount of contradiction.

Statistical comparison between MISR and MODIS/Terra AOD at corresponding AERONET stations is performed by calculating G-fraction using $\Delta\tau = \pm 0.05 \pm 0.15\tau_{AERO}$ as a confidence interval. Over the region 1, MISR AOD retrievals are more accurate than MODIS retrievals. MODIS, however, performs better over region 2 sites with high percentage of the data points falling within the confidence range (Tables 2 and 3). High light reflections from the desert landscape surrounding region 1 could have an effect on MODIS retrievals.

Excluding Bahrain and Cairo for low data retrievals the performance of MODIS tends to be similar over all region with ~ 64 percent of AOD retrievals fall within the $\Delta\tau = \pm 0.05 \pm 0.15\tau_{AERO}$ confidence range of the AERONET AOD while MISR retrievals show better performance with ~ 84 percent of the data falling within the same confidence range. This could be attributed to low number of retrievals available for Bahrain and Cairo compared to other sites. Vast sea region surrounding Bahrain and complex landscape in Cairo could also have an impact on retrievals.

4.3 Evaluating the MISR and MODIS climatology over Middle East and North Africa

Comparisons between MISR and MODIS AOD at selected AERONET stations over the 2000 – 2015 period are shown in Figures 6- 12.

Figure (6a, b) shows histogram of the MISR, MODIS and AERONET AOD at Solar Village for MISR and MODIS data points collocated with AERONET observations. The mean, standard deviation, and number of measurements are also presented.

MISR tends to underestimate the frequency of low AOD compared to AERONET but overestimate the frequency of high AOD. MISR histograms show prominent peaks at 0.50 that can be also observed in AERONET and at 0.75 that could not be seen in AERONET. MISR and AERONET AOD climatology agree well with one another. MODIS also tends to underestimate the frequency of low AOD events and overestimate the frequency of high AOD events. High surface reflectance could cause overestimation in MODIS AOD (Ichoku et al., 2005). Both MISR and MODIS provide a good representation of the AOD climatology as compared to AERONET at the Solar Village. Mezaria station, which is located in an arid region in the UAE, has a similar climatology to the Solar Village site with dust dominating aerosol. Figure (7a, b) shows histograms of the MISR, MODIS and AERONET AOD at Mezaria.

Similar to the Solar Village, there is a big difference between the number of samples in the matched data set and full AERONET climatology. For MISR there are 213 matched cases and for MODIS there are 498 compared to the 2245 for the entire site. This has an impact on the overall assessment showing significant differences between the matched data and the full climatology for both MISR and MODIS. First, for the MISR case, the matched AERONET data have the highest frequency at AOD of 0.15 and 0.35, but the climatology shows the highest frequency at an AOD of 0.25. AOD in the range of 0.25 to 0.30 are undersampled relative to the climatology, and AOD more than 0.35 matches the climatology with less than 2 percent AOD greater than 0.85. MODIS matched AERONET data show prominent peaks at 0.3 and 0.4 compared to the climatology that has a single peak at 0.30.

For AOD values between 0.25 and 0.40 MODIS data were found to be under-sampled similar to MISR data between 0.65 to 0.70 and at 0.35.

MISR AOD retrievals matched to AERONET capture the variability in the distribution, but as in the case of Solar Village the frequency of low AOD events is underestimated but the frequency of high AOD events matched AERONET data. MISR also captures events with AOD greater than 1. A similar situation is seen in the MODIS comparison, but MODIS appears to do a better job capturing the overall shape of the AERONET AOD histogram for this site.

The Bahrain AERONET site is located in Manama fairly close to the Arabian Gulf, a location very different from the previous two sites. The site is also located in an urban area suffers from significant load of anthropogenic aerosols as a consequence of rapid aluminium industrial development (Farahat 2016). Figure (8a, b) shows histogram of the MISR, MODIS and Bahrian AERONET measurements with statistical analysis displayed. The AERONET data matched to MISR show significant peaks at 0.20, 0.30, 0.45, 0.55, 0.7, 0.8, and 0.95 not seen in the all data climatology that has peaks at 0.55 and 0.70. AOD less than 0.15 are not representative in the matched data set at all. MISR is representing the peaks at 0.45 in the matched data set but misses the peaks at 0.20, 0.30, and 0.35. The MISR climatology agrees well with the AERONET all data climatology for all AOD. MODIS on the other hand shows an extremely large frequency of AOD at 0.1 not represented by AERONET coupled with an underestimation of AOD greater than 0.3. This could be attributed to the size of the matching window and MODIS retrievals preferentially coming from the Arabian Gulf.

SAADA station is located close to some hiking trails at the Agoundis Valley in the Atlas Mountains about 197 km from the city of Marrakesh.

MISR AOD matched to AERONET agree well with MISR full climatology retrievals over SAADA station. Both retrievals slightly underestimate SAADA full climatology and over estimate SAADA matched data retrievals at AOD equal to 0.2 while show good agreement for AOD greater than 0.2. MODIS matched to AERONET retrievals overestimate the frequency of AOD greater than 0.3. While MODIS AOD matched to AERONET captures climatology at AOD between 0.2 to 0.25, AOD frequency retrievals are under-sampled at

AOD between 0.1 to 0.15 with about 13 % less events than SAADA all data retrievals at AOD equal to 0.1.

Figure (9a, b) indicates right skewed distribution of SAADA AOD towards small AOD values with 10.3 % and 30.1 % of AOD > 0.4 as measured by MISR and MODIS respectively. Taking into consideration MODIS overestimation we conclude that SAADA site is characterized by small AOD values and this could be related to the land topology where the station is located.

While MISR is capturing high AOD climatology over SAADA, both MISR and MODIS are underestimating the frequency of lower AOD events. Nevertheless, MISR captures the climatology of AOD less than 0.1 missed by MODIS retrievals.

Taman AERONET station is located at the oasis city of Tamanrasset, which lies in Ahaggar National Park in southern Algeria.

Figure (10 a, b) depicts that Taman AERONET AOD climatology is similar to those at SAADA and has a high frequency of low AOD events. Both MISR AOD matched to AERONET and MISR all data do not well capture the frequency of AOD less than 0.1 or larger than 1 while well describe the climatology for AOD in the range of 0.1 to 1. MODIS AOD matched data to AERONET correctly describe climatology with slight overestimation of AOD frequencies between 0.05 – 0.15 while not capturing AOD frequencies greater than 1. MISR and MODIS show similar prominent peaks at 0.1 and 0.25 not observed in Taman AERONET AOD climatology, with more peaks observed by MISR at 0.5, 0.75, and 0.85. Average AOD in SAADA and Taman is ~ 50 percent less than observed at Solar Village, Mezaria, and Bahrain sites.

Except for AOD greater than 1 where ground observations could be more robust, both MISR and MODIS retrievals can provide very good climatology matching over Taman site.

Taking into consideration lower number of MISR matching AERONET observations compared to MODIS ~ 21 and 49 percent over SAADA and Taman respectively, MISR is outperforming over these two sites, which can be attributed to its multiangle viewing capabilities over complex terrains including mountainous areas (Atlas Mountains).

Cairo is a mega city well known for its high pollution due to traffic and agriculture activities. MISR and MODIS matched data correctly capture AOD climatology over Cairo compared to AERONET as shown in Figure (11a, b). MISR retrievals collocated with AERONET over estimate prominent peaks of AERONET AOD at 0.15 – 0.35 while underestimate AERONET AOD greater than 0.35. MISR 'all data' AOD climatology over Cairo station agrees better with AERONET AOD climatology vs. collocated dataset with some oversampling at 0.25. Frequency of high AOD retrievals greater than 0.8 have not been captured by MISR matched or all data retrievals. MODIS matched to AERONET AOD are also able to well represent Cairo climatology data with a high overestimation of AOD frequency between 0.05 - 0.2 and an underestimation of AOD larger than 0.4.

The complex landscape and local emissions in Cairo could impose major challenges in MODIS AOD retrievals. Moreover, Cairo is one of the most densely populated cities in the world that hosts major commercial and industrial centers in North Africa. Cairo also has complicated aerosols structure developed by long range transported dust in the spring, biomass burning in the fall, strong traffic and industrial emissions (Marey et al., 2010).

Over Cairo station, MODIS correctly represents ground observations for AOD between 0.2 - 0.4 while MISR all data better represents AOD climatology for AOD greater than 0.4.

MISR, MODIS climatology at SEDEE Boker are illustrated in Figures (12a, b).

MISR 'matched' AOD frequency show significant underestimation for AOD less than 0.2 and an overestimation between 0.2 – 0.4 compared with AERONET retrievals. MISR correctly captures the climatology for AOD events greater than 0.4. MISR ‘matched’ and ‘all data’ retrievals peaks at 0.2 producing high frequency of AOD oversampling compared to AERONET. MISR data retrievals do not capture the climatology for AOD less than 0.1 over this site coincident with what was previously observed over other sites. MODIS matched AERONET data underestimates frequency of AOD less than 0.2 while overestimates the frequencies between 0.2 - 0.6, and well match frequencies of higher AOD events larger than 0.6. MODIS retrievals are characterized by two prominent peaks at 0.1 and 0.25 that are not found in the AERONET matched data.

At Sedee, MISR and MODIS retrievals are better in matching frequency of high AOD retrievals (greater than 0.4) than the frequency of low AOD. This could be an effect of possible long-range transport to Sedee Boker site (Farahat et al. 2016) along with complex mixtures of dust, pollution, smoke, and sea salt that could result in uncertainties in MISR and MODIS aerosol model selection.

In the summary, MISR tends to overestimate AOD > 0.4 over Solar Village, Bahrain and underestimate AOD > 0.4 over Cairo. MISR retrievals also match AOD > 0.4 for Mezaria and Sedee Boker, while agree with AERONET over SAADA and Taman at all ranges of AOD. This could be expounded by insufficient particle absorption in MISR algorithm (Kahn et al., 2005). Spherical particle absorption is produced by externally mixing small black carbon particles.

Percentage of MISR, MODIS, and AERONET AOD greater than 0.4 recorded is shown in Table 4. Over Solar Village, both MISR and MODIS well capture high AOD greater than 0.4 with very good agreement with the ground observations. Over Mezaria, both MISR and MODIS are over estimating the percentage of AOD greater than 0.4 by about 17.7 and 12.7 percent respectively. MISR all data agrees well with AERONET all data in representing high AOD over Bahrain while MODIS shows significant under-representation of those events by about 13 percent, less than reported by Bahrain AERONET station. At SAADA, MISR AOD agrees with AERONET in showing low percentage of AOD greater than 0.4, while MODIS retrievals overestimate percentage by about 24 percent. MISR AOD over Taman AERONET station shows very good agreement, while MODIS is slightly underestimating AOD. Among all seven sites considered in this study, Sedee Boker shows lowest occurrence of AOD greater than 0.4, which is confirmed by both MISR and MODIS retrievals. Cairo AERONET records the highest frequency of AOD > 0.4, however this is largely underestimated by both MISR and MODIS retrievals.

It can be concluded from the previous discussion that the atmosphere around SAADA, Taman, and Sedee Boker sites is relatively clean and aerosol loads are small compared to Solar Village, Mezaria, Bahrain, and Cairo, however this could be affected by the location where AERONET station is installed for example SAADA and Taman stations are installed in a remote mountainous region away from urbanization while Cairo station is installed in the middle of large residential region with significant local emissions.

Conclusion

The performance of MODIS, MISR retrievals with corresponding AERONET measurements over different geographic locations in the Middle East and North Africa was investigated during 2000 – 2015.

Long-term observations show dissimilar AOD trends between MODIS/Aqua, MODIS/Terra, MISR and AERONET measurements. MODIS/Aqua matched AERONET retrievals show stable trend over all sites while, MODIS/Terra matched AERONET retrievals show significant downward trend indicating possible changes in the sensor performance.

MISR matched AERONET AOD data depict high correlation compared to AERONET indicating good agreement with ground observations with about 84 percent of AOD retrievals fall within the expected confidence range.

Consistency of MODIS and AERONET AOD vary based on the season, study area, and dominant aerosols type with about 64 percent of the retrieved AOD values fall within expected confidence range with the lowest performance over mixed particles regions.

Comparing satellites' AOD retrievals with corresponding AERONET measurements show that space-borne data retrievals accuracy can be affected by landscape, topology, and AOD range at which data is retrieved.

Few AERONET sites are verified where MISR and MODIS retrievals agree well with ground observations, while other sites only MISR or MODIS could correctly describe the climatology.

The AOD range at which MISR or MODIS could correctly describe ground observation is also investigated over different AERONET sites. Over Solar Village both MISR and MODIS tend to underestimate the frequency of low AOD and overestimate the frequency of high AOD compared to AERONET with MISR histograms show prominent peaks at 0.50 that matched AERONET data and 0.75 that could not be recorded in AERONET. MISR can capture the frequency of AOD greater than 1 mostly missed by MODIS. Both MISR and MODIS are found to provide good representation of the AOD climatology over the Solar Village site.

Similar to Solar Village, MISR underestimates frequency of lower AOD and overestimate frequencies of high AOD over Mezaria. MISR is able to correctly capture the frequency of AOD greater than 1, while MODIS retrievals are found to better represent the overall climatology. This is due to low number of MISR – matched AERONET retrievals compared to MODIS over this site. Prominent peaks at 0.3 and 0.4 were observed in MODIS matched Mezaria retrievals compared to the climatology, which has a single peak at 0.30.

Large water body surrounding Bahrain makes MODIS data preferentially originate from the Arabian Gulf which produces an extremely large frequency of AOD at 0.1 not observed in AERONET measurements paired with an underestimation of AOD greater than 0.3. Meanwhile, MISR retrievals agree well with AOD climatology over Bahrain.

MISR AOD retrievals slightly underestimate SAADA climatology while they show good agreement for AOD greater than 0.1. MODIS retrievals underestimate the frequency of AOD retrievals between 0.1 to 0.15, match climatology at AOD between 0.2 to 0.25, and overestimate the frequency of AOD greater than 0.3. SAADA site is characterized by small frequency of low AOD values and this could be related to the landscape nature surrounding Saada station. MISR is found to be outperforming over Saada and Taman stations which can be attributed to its viewing multispectral and multiangular capabilities over mountainous regions.

MISR retrievals well capture prominent peaks of AERONET data at 0.15 to 0.35 with small underestimation observed at AOD greater than 0.3 over Cairo. Using either MISR matched data or MISR all data over Cairo was found to perform well in describing the climatology over this station. MODIS data retrievals are also able to well represent Cairo climatology with a high overestimation of AOD frequency between 0.05 to 0.2 and an underestimation of AOD larger than 0.4. While both MISR and MODIS well describe climatology over Cairo station, MODIS can correctly represent ground observations between 0.2 to 0.4.

Over Sedee Boker both MISR and MODIS retrievals well describe the climatology however they are more successful in matching frequency of high AOD greater than 0.4.

Based on analysing frequency of AOD greater than 0.4, it was found that Saada, Taman, and Sedee Boker are having better air quality compared to other sites while Cairo was found to be the most polluted site.

Results presented in this study are important in providing a guideline for satellites retrievals end users on which sensor could provide reliable data over certain geographic location and AOD range.

Adjacent geographic location and local climate among sites does not always guarantee that same sensor will provide consistent retrievals over all sites. For example, Solar Village, and Bahrain AERONET are surrounded by large desert regions and sharing almost similar climatic conditions, but MODIS is found to be more successful in describing climatology over Solar Village than over Bahrain and this could be attributed to different factors related to surface reflection, cloud coverage, and the large water body surrounding Bahrain. Thus in order to decrease data uncertainty, it is important to determine which sensor provides best retrieval over certain geographic location and AOD range.

Acknowledgements

The author would like to acknowledge the support provided by the Deanship of Scientific Research (DSR) at the King Fahd University of Petroleum and Minerals (KFUPM) for funding this work through project # IN161053. Portions of this work were performed at the Jet Propulsion Laboratory (JPL), California Institute of Technology, under a contract with the National Aeronautics and Space Administration. The author would like to thank Michael Garay (MJG) and Olga Kalashnikova (OVK) (JPL) for their suggestion of investigating satellites – AERONET matched data climatology, and discussion during the data analysis. The author would also like to thank Hesham El-Askary (Chapman University) for providing recommendation about AERONET data over North Africa and the Middle East as well as reviewing the English in the manuscript. We thank the MISR project for providing facilities, and supporting contributions of MJG and OVK. Finally, we thank the reviewers for suggestions, which improved the manuscript.

Author Contributions: Ashraf Farahat analysed the data, performed the statistical analysis and wrote the manuscript.

Conflicts of Interest: The authors declare no conflict of interest.

References

1. Abdi, V., Flamant, C., Cuesta, J., Oolman, L., Flamant, P., and Khalesifard. H. R. Dust transport over Iraq and northwest Iran associated with winter Shamal: A case study. J. Geophys. Res., 117, D03201, 2013.

2. Ackerman, S., Strabala, K. I., Menzel, W. P., Frey, R. A., Moeller, C. C. and Gumley, L. E. (1998): Discriminating clear sky from clouds with MODIS. J. Geophys. Res., 103, 32 141–157, 1998.

3. Afnan, F. Heavy metal, trace element and petroleum hydrocarbon pollution in the Arabian Gulf: Review, Journal of the Association of Arab Universities for Basic and Applied Sciences, 17, 90-100, 2015.

4. Ansmann, A., Petzold, A., Kandler, K., Tegen, I., Wendisch, M., Müller, D., Weinzierl, B., Müller, T., and Heintzenberg, J. Saharan Mineral Dust Experiments SAMUM-1 and SAMUM-2: what have we learned? Tellus B, 63, 403–429, 2011.

5. Basart, S., Pérez, C., Cuevas, E., Baldasano, J. M., and Gobbi., G. P. Aerosol characterization in Northern Africa, Northeastern Atlantic, Mediterranean Basin and Middle East from direct-sun AERONET observations. Atmos. Chem. Phys., 9, 8265-8282, 2009.

6. Böer B., An introduction to the climate of the United Arab Emirates (review). J Arid Environ, 35:3–16, 1997.

7. Bou Karam, D., Flamant, C., Cuesta, J., Pelon, J., and Williams, E. Dust emission and transport associated with a Saharan depression: February 2007 case, J. Geophys. Res., 115, D00H27, 2010.

8. Bre´on, F-M., Vermeulen, A., Descloitres, J. An evaluation of satellite aerosol products against sunphotometer measurements. *Remote Sensing Environ.*, 115, 3102–11, 2011.

9. Bruegge, C., Chrien, N., Kahn, R., Martonchik, J., and Diner, D. MISR radiometric uncertainty analyses and their utilization within geophysical retrievals. *IEEE Trans. Geosci. Remote Sens.*, 36, 1186- 1198, 1998.

10. Chin, M., Diehl, T., Tan, Q., Prospero, J. M., Kahn, R. A., Remer, L. A., Yu, H., Sayer, A. M., Bian, H., Geogdzhayev, I. V., Holben, B. N., Howell, S. G., Huebert, B. J., Hsu, N. C., Kim, D., Kucsera, T. L., Levy, R. C., Mishchenko, M. I., Pan, X., Quinn, P. K., Schuster, G. L., Streets, D. G., Strode, S. A., Torres, O., and Zhao, X.-P. Multi-decadal aerosol variations from 1980 to 2009: a perspective from observations and a global model, Atmos. Chem. Phys., 14, 3657-3690, 2014.

11. Chu, D. A., Kaufman, Y. J., Remer, L. A., and Holben, B. N. Remote sensing of smoke from MODIS airborne simulator during the SCAR-B experiment. J. Geophys. Res., 103, 31, 979– 987, 1998.

12. Derimian, Y., Karnieli, A., Kaufman, Y. J., Andreae, M. O., Andreae, T. W., Dubovik, O., Maenhaut, W., Koren, I., and Holben, B. N. Dust and pollution aerosols over the Negev desert, Israel: Properties, transport, and radiative effect. J. Geophys. Res., 111, D05205, 2006.

13. Dubovik, O. and King, M. D. A flexible inversion algorithm for retrieval of aerosol optical properties from Sun and sky radiance measurements. J. Geophys. Res., 105 206730–20696, 2000.

14. Dubovik, O., Holben, B. N., Eck, T. F., Smirnov, A., Kaufman, Y. J., King, M. D. Tanre, D., and Slutsker, I. Variability of absorption and optical properties of key aerosol types observed in worldwide locations. J. Atmos. Sci., 59, 590–608, 2002.

15. Dubovik, O., Sinyuk, A., Lapyonok, T., Holben, B., Mischenko, M.,Yang, P., Eck, T., Volten, H., Muñoz, O., Veihelmann, B., van der Zande, W. J., Leon, J.-F., Sorokin, M., and Slutsker, I. The application of spheroid models to account for aerosol particle non-sphericity in remote sensing of desert dust. J. Geophys. Res., 111, D11208, 2006.

16. Eck, T., Holben, B. N., Reid, J. S., O'Neill, N. T., Schafer, J. S., Dubovik, O., Smirnov, A., Yamasoe, M. A., and Artaxo, P. High aerosol optical depth biomass burning events: A comparison of optical properties for different source regions, Geophys. Res. Lett., 200b, 30, 20, 2035, 2003b.

17. Eck, T., et al. Climatological aspects of the optical properties of fine/coarse mode aerosol mixtures. J. Geophys. Res., 115, D19205, 2010.

18. Elagib, N., Addin Abdu A. Climate variability and aridity in Bahrain. J. Arid Environ., 36:405–419, 1997.

19. El-Askary H., Farouk R., Ichoku C., and Kafatos M. Inter-continental transport of dust and pollution aerosols across Alexandria, Egypt, Annales Geophysicea, 27, 2869–2879, 2009.

20. Farahat, A., El-Askary, H., and Al-Shaibani, A. Study of Aerosols' Characteristics and Dynamics over the Kingdom of Saudi Arabia using a Multi Sensor Approach Combined with Ground Observations. Advances in Meteorology, Article ID 247531, 2015.

21. Farahat, A. Air Pollution in Arabian Peninsula (Saudi Arabia, United Arab Emirates, Kuwait, Qatar, Bahrain, and Oman): Causes, Effects and Aerosol Categorization. Arab J of Geosci., 9, 196, 2016.

22. Farahat, A., El-Askary, H., and Dogan, A. U., 2016: Aerosols size distribution characteristics and role of precipitation during dust storm formation over Saudi Arabia. Aerosol Air Qual. Res., 16, 2523-2534, 2016.

23. Farahat, A., El-Askary, H., Adetokunbo, P., Abu-Tharr, F. Analysis of aerosol absorption properties and transport over North Africa and the Middle East using AERONET data. Annales Geophysicae., 34:11, 1031-1044, 2016.

24. He, Q., Li, C., Tang, X., Li, H., Geng, F., Wu, Y. Validation of MODIS derived aerosol optical depth over the Yangtze River Delta in China. Remote Sensing Environ., 114, w21649–61, 2010.

25. Higurashi, A., and Nakjima, T. Development of a two-channel aerosol retrieval algorithm on a global scale using NOAA AVHRR. J. Atmos. Sci., 56, 924–941, 1999.

26. Holben, B., Eck, T., Slutsker, I., Tanre, D., Buis, J., Setzer, A. et al. AERONET—A federated instrument network and data archive for aerosol characterization. Remote Sensing Environ., 66, 1–16, 1998.

27. Holben, B., Smirnov, A., Eck, T., Slutsker, I., Abuhassan, N., Newcomb, W., et al. An emerging ground-based aerosol climatology—Aerosol optical depth from AERONET, J. Geophys Res., 106, 12067–97, 2001.

28. Hoell, A., Funk, C., and Barlow, M. The regional forcing of Northern Hemisphere drought during recent warm tropical west Pacific Ocean La Niña events. Clim. Dyn., 42, 3289–3311, 2013.

29. Hsu, N., Gautam, R., Sayer, A., Bettenhausen, C., Li, C., Jeong, M., Tsay, S., and Holben, B. Global and regional trends of aerosol optical depth over land and ocean using SeaWiFS measurements from 1997 to 2012. Atmos. Chem. Phys., 12, 8037–8053, 2012.

30. Ichoku, C., Chu, D. A., Mattoo, S., Kaufman, Y. J., Remer, L. A., Tanre, D., Slutsker, I., and Holben, B. N. A spatio-temporal approach for global validation and analysis of MODIS aerosol product, Geophys. Res. Lett., 29, 12, 8006, 2002.

31. Ginoux, P., Chin, M., Tegen, I., Prospero, J., Holben, B., Dubovik, O., and Lin, S.-J. Sources and global distributions of dust aerosols simulated with the GOCART model, J. Geophys. Res., 106, 20255 – 20273, 2001.

32. Kahn, R. A., Gaitley, B. J., Martonchik, J. V., Diner, D. J., Crean, K. A. and Holben, B. Multiangle ImagingSpectroradiometer (MISR) global aerosol optical depth validation based on 2 years of coincident Aerosol Robotic Network (AERONET) observations, J. Geophys. Res., 110, 2005.

33. Kahn, R., Garay, M., Nelson, D., Yau, K., Bull, M., Gaitley, B. et al. Satellite-derived aerosol optical depth over dark water from MISR and MODIS: Comparisons with AERONET and implications for climatological studies. J. Geophys. Res., 112, D18205, 2007.

34. Kahn, R., Nelson, D., Garay, M., Levy, R., Bull, M., Diner, D., et al. MISR aerosol product attributes, and statistical comparisons with MODIS. IEEE Trans Geosci Remote Sensing, 47, 4095–114, 2009.

35. Kim, D., Chin, M., Bian, H., Tan, Q., Brown, M. E., Zheng, T., You, R., Diehl, T., Ginoux, P., and Kucsera, T. The effect of the dynamic surface bareness on dust source function, emission, and distribution, J. Geophys. Res., 118, 1–16, 2013.

36. Kaufman, Y., Tanre, D., Remer, L., Vermote, E., Chu, A., and Holben, B. Operational remote sensing of tropospheric aerosol over land from EOS moderate resolution imaging spectroradiometer. J. Geophys. Res.-Atmos., 102, D14, 17051–17067, 1997.

37. Kokhanovsky, A., Breon, F., Cacciari, A., Carboni, E., Diner, D., Di Nicolantonio, W. et al. Aerosol remote sensing over land: a comparison of satellite retrievals using different algorithms and instruments. Atmos Res., 85, 372–94, 2007.

38. Liu, L., Mishchenko. M. Toward unified satellite climatology of aerosol properties: direct comparisons of advanced level 2 aerosol products. JQSRT., 109, 2376–85, 2008.

39. Marey, H., Gille, J., El-Askary, H., Shalaby, E. , and El- Raey, M. Study of the formation of the “black cloud and its dynamics over Cairo, Egypt, using MODIS and MISR sensors. *J. Geophys. Res*., 115, D21206, 2010.

40. Martonchik, J., Diner, D., Crean, K., and Bull. M. Regional aerosol retrieval results from MISR. IEEE Trans. Geosci. Remote Sens., 40, 1,520–1,531, 2002.

41. Mishchenko, M., I. Geogdzhayev, L. Liu, A. Lacis, B. Cairns, L. Travis. Toward unified satellite climatology of aerosol properties: what do fully compatible MODIS and MISR aerosol pixels tell us? J Quant Spectrosc Radiat Transfer. 110, 402–8, 2009.

42. Mishchenko, M., Liu, L., Geogdzhayev, I., Travis, L., Cairns, B., Lacis, A. Toward unified satellite climatology of aerosol properties: 3. MODIS versus MISR versus AERONET. J Quant Spectrosc Radiat Transfer., 111, 540–52, 2010.

43. Remer, L., Kaufman, Y., Tanre´, D., Mattoo, S., Chu, D., Martins, J., et al. The MODIS aerosol algorithm, products, and validation. J Atmos Sci., 62, 947–73, 2005.

44. Sadiq, M. and McCain, J. The Gulf War Aftermath: An Environmental Tragedy., 1st ed., Springer, 1993.

45. Sayer, A., Hsu, N., Eck, T., Smirnov, A., and Holben, B. AERONET-based models of smoke-dominated aerosol near source regions and transported over oceans, and implications for satellite retrievals of aerosol optical depth. Atmos. Chem. Phys., 14, 11493-11523, 2014.

46. Schepanski, K., Mallet, M., Heinold, B., and Ulrich, M.: North African dust transport toward the western Mediterranean basin: atmospheric controls on dust source activation and transport pathways during June–July 2013, Atmos. Chem. Phys., 16, 14147-14168, 2016.

47. Sioris, C. E., McLinden, C. A., Shephard, M. W., Fioletov, V. E., and Abboud, I.: Assessment of the aerosol optical depths measured by satellite-based passive remote sensors in the Alberta oil sands region, Atmos. Chem. Phys., 1931-1943, 2017.

48. Smirnov, A., Holben, B., Eck, T., Dubovik, O., and Slutsker, I. Cloud-screening and quality control algorithms for the AERONET data-base, Remote Sens. Environ., 73, 337 – 349, 2000**.**

49. Solomos, S., Ansmann, A., Mamouri, R.-E., Binietoglou, I., Patlakas, P., Marinou, E., and Amiridis, V. Remote sensing and modelling analysis of the extreme dust storm hitting the Middle East and eastern Mediterranean in September 2015, Atmos. Chem. Phys., 17, 4063-4079, 2017.

50. Todd M., R. Washington, Vanderlei, M., Dubovik, O., Lizcano, G., M'Bainayel, S., Engelstaedter, S. Mineral dust emission from the Bodélé Depression, northern Chad, during BoDEx 2005. J. Geophys. Res., 112. D06207, 2007.

51. Von Hoyningen-Huene, W., Posse, P. Nonsphericity of aerosol particles and their contribution to radiative forcing. JQSRT, 57, 651–68, 1997.

52. Yu, Y., Notaro, M., Liu, Z., Kalashnikova, O., Alkolibi, F., Fadda, E., and Bakhrjy, F. Assessing temporal and spatial variations in atmospheric dust over Saudi Arabia through satellite, radiometric, and station data, J. Geophys. Res. Atmos., 118, 13, 253–13, 264, 2013.

53. Yu, Y., Notaro, M., Liu, Z., Wang, F., Alkolibi, F., Fadda, E. and Bakhrjy, F. Climatic controls on the interannual to decadal variability in Saudi Arabian dust activity: Toward the development of a seasonal dust prediction model. J. Geophys. Res. Atmos., 120, 1739–1758, 2015.

54. Zhao, G. and Girolamo, L. A cloud fraction versus view angle technique for automatic in-scene evaluation of the MISR cloud mask. J. Appl. Meteorol., 43, 6, 860–869, 2004.

Tables' caption

Table 1. Geographic location of the AERONET sites used in this study

Table 2. Statistics for dust sites, R: correlation coefficient, RMSE: Root Mean Square deviation; G-fraction: good fraction; N: number of observations

Table 3. Statistics for biomass and mixed sites, parameters as in Table 3. Caption.

Table 4. MISR coverage for six days of major dust activity over the Arabian Peninsula during March 2009.

Figures caption

Figure 1. Location of the AERONET stations over North Africa and the Middle East. The numbers on the map indicates the site location as 1: Saada, 2: Tamanrasset_INM, 3: Cairo, 4: Sede Boker, 5: Solar Village, 6: Mezaira, 7: Bahrain.

Figure 2. Scatter plot of MISR AOD versus AERONET AOD based on seasons and aerosols categorization.

Figure 3. Scatter plot of MODIS AOD versus AERONET AOD based on seasons and aerosols categorization.

Figure 4. Time series of monthly mean AOD derived from MODIS/Aqua, MODIS/Terra, MISR and AERONET over a) dust b) biomass and c) mixed dominated aerosol regions.

Figure 5. Long-term AOD difference for MODIS/Terra and MODIS/Aqua over the Solar Village and Taman sites.

Figure 6. Histogram of the MISR, MODIS and Solar Village AERONET measurements a) MISR b) MODIS data retrievals.

Figure 7. Histogram of the MISR, MODIS and Mezaria AERONET measurements a) MISR b) MODIS data retrievals.

Figure 8. Histogram of the MISR, MODIS and Bahrain AERONET measurements a) MISR b) MODIS data retrievals.

Figure 9. Histogram of the MISR, MODIS and SAADA AERONET measurements a) MISR b) MODIS data retrievals.

Figure 10. Histogram of the MISR, MODIS and Taman AERONET measurements a) MISR b) MODIS data retrievals.

Figure 11. Histogram of the MISR, MODIS and SEDEE Boker AERONET measurements a) MISR b) MODIS data retrievals.

Figure 12. Histogram of the MISR, MODIS and Cairo AERONET measurements a) MISR b) MODIS data retrievals.

Table 1.

Location name	Lon./Lat.	Measurement period
Solar Village	24.907° N/46.397° E	2000-2015
Mezaria	23.105° N/53.755° E	2004-2015
Bahrain	26.208° N/50.609° E	2000-2006
Saada	31.626° N/8.156° W	2003-2015
Taman	22.790° N/5.530° E	2000-2015
Cairo (EMA_2)	30.081° N/31.290° E	2010 -2017
Sede Boker	30.855° N/34.782 ° E	2000-2015

Table 2.

AERONET Site	Sensor	Season	Mean Value		N	R	Gfraction (%)
			AERONET	Satellite			
Solar Village	MISR	DJF	0.18±0.15	0.23±0.13	24	0.94	79.1
		MAM	0.45±0.21	0.47±0.20	43	0.94	86.0
		JJA	0.39±0.16	0.42±0.16	57	0.90	82.4
		SON	0.25±0.14	0.29±0.12	50	0.99	82.0
	MODIS Terra	DJF	0.27±0.19	0.33±0.17	1500	0.48	51.80
		MAM	0.36±0.24	0.26±0.17	389	0.68	90.23
		JJA	0.34±0.17	0.42±0.19	429	0.41	54.31
		SON	0.22±0.10	0.36±0.12	471	0.51	28.87
Mezaria	MISR	DJF	0.17±0.09	0.23±0.07	53	0.89	50.9
		MAM	0.34±0.18	0.37±0.18	41	0.90	78.0
		JJA	0.49±0.20	0.47±0.21	51	0.85	92.1
		SON	0.26±0.09	0.30±0.12	53	0.87	88.2
	MODIS Terra	DJF	0.32±0.15	0.35±0.19	198	0.86	74.74
		MAM	0.44±0.33	0.45±0.27	115	0.92	78.07
		JJA	0.39±0.14	0.43±0.20	89	0.81	71.91
		SON	0.28±0.13	0.30±0.16	97	0.87	77.31
Bahrain	MISR	DJF	0.19±0.10	0.30±0.10	9	0.73	33.3
		MAM	0.47±0.20	0.67±0.05	7	0.89	28.5
		JJA	0.45±0.21	0.74±0.21	21	0.69	23.8
		SON	0.32±0.13	0.45±0.16	22	0.98	45.4
	MODIS Terra	DJF	0.42±0.29	0.20±0.19	121	0.41	93.38
		MAM	0.50±0.28	0.13±0.15	25	0.26	96.00
		JJA	0.55±0.26	0.31±0.27	42	0.50	88.09
		SON	0.35±0.14	0.21±0.12	29	0.32	93.10

Table 3.

AERONET Site	Method	Season	Mean Value		N	R	Gfraction (%)
			AERONET	Satellite			
SAADA	MISR	**DJF**	0.07±0.02	0.07±0.02	43	0.93	100.0
		MAM	0.17±0.10	0.17±0.09	47	0.89	93.6
		JJA	0.30±0.14	0.31±0.14	53	0.93	93.1
		SON	0.14±0.07	0.13±0.06	51	0.94	96.0
	MODIS Terra	**DJF**	0.23±0.16	0.32±0.21	550	0.57	57.8
		MAM	0.24±0.18	0.39±0.23	90	0.43	44.4
		JJA	0.30±0.17	0.45±0.18	201	0.40	45.2
		SON	0.19±0.13	0.22±0.14	162	0.71	72.3
Taman	MISR	**DJF**	0.07±0.10	0.09±0.06	69	0.92	85.5
		MAM	0.22±0.18	0.25±0.22	86	0.97	81.3
		JJA	0.42±0.31	0.45±0.28	57	0.85	78.9
		SON	0.14±0.11	0.15±0.10	72	0.94	95.8
	MODIS Terra	**DJF**	0.19±0.22	0.18±0.16	319	0.67	81.8
		MAM	0.24±0.19	0.22±0.17	67	0.55	83.5
		JJA	0.37±0.32	0.29±0.20	69	0.69	84.0
		SON	0.14±0.14	0.13±0.10	117	0.54	84.6
Cairo	MISR	**DJF**	0.33±0.17	0.17±0.09	15	0.94	100.0
		MAM	0.35±0.13	0.33±0.15	39	0.99	82.0
		JJA	0.35±0.09	0.27±0.08	61	0.99	967
		SON	0.37±0.14	0.28±0.13	23	0.97	78.2
	MODIS Terra	**DJF**	0.33±0.16	0.20±0.11	158	0.30	95.5
		MAM	0.32±0.16	0.12±0.08	39	0.25	100.0
		JJA	0.35±0.14	0.28±0.07	58	0.17	94.8
		SON	0.38±0.19	0.20±0.09	29	0.07	93.8

SEDEE_BOKER	**MISR**	**DJF**	0.11±0.06	0.13±0.05	10	0.87	90.0
		MAM	0.21±0.13	0.24±0.13	76	0.68	75.0
		JJA	0.16±0.08	0.21±0.08	142	0.85	66.9
		SON	0.162±0.07	0.20±0.06	54	0.89	79.6
	MODIS Terra	**DJF**	0.16±0.12	0.23±0.14	1312	0.36	53.5
		MAM	0.21±0.18	0.24±0.19	338	0.34	65.6
		JJA	0.16±0.09	0.33±0.13	392	0.27	17.3
		SON	0.16±0.09	0.23±0.12	477	0.46	58.4

Table 4.

	AERONET		MISR		MODIS	
		AOD		AOD		AOD
	N	% > 0.4	N	% > 0.4	N	% > 0.4
Solar Village	3893	27.17	684	32.8	2789	30.1
Mezaria	2245	28.01	547	45.7	498	40.7
Bahrain	1116	31.36	676	35.8	217	18.4
SAADA	2974	10.32	667	11.5	1004	34.6
Taman	798	15.78	845	22.6	572	9.4
Cairo	2222	38.79	620	17.7	284	4.2
SEDEE	5722	4.28	675	9.0	2519	12.8

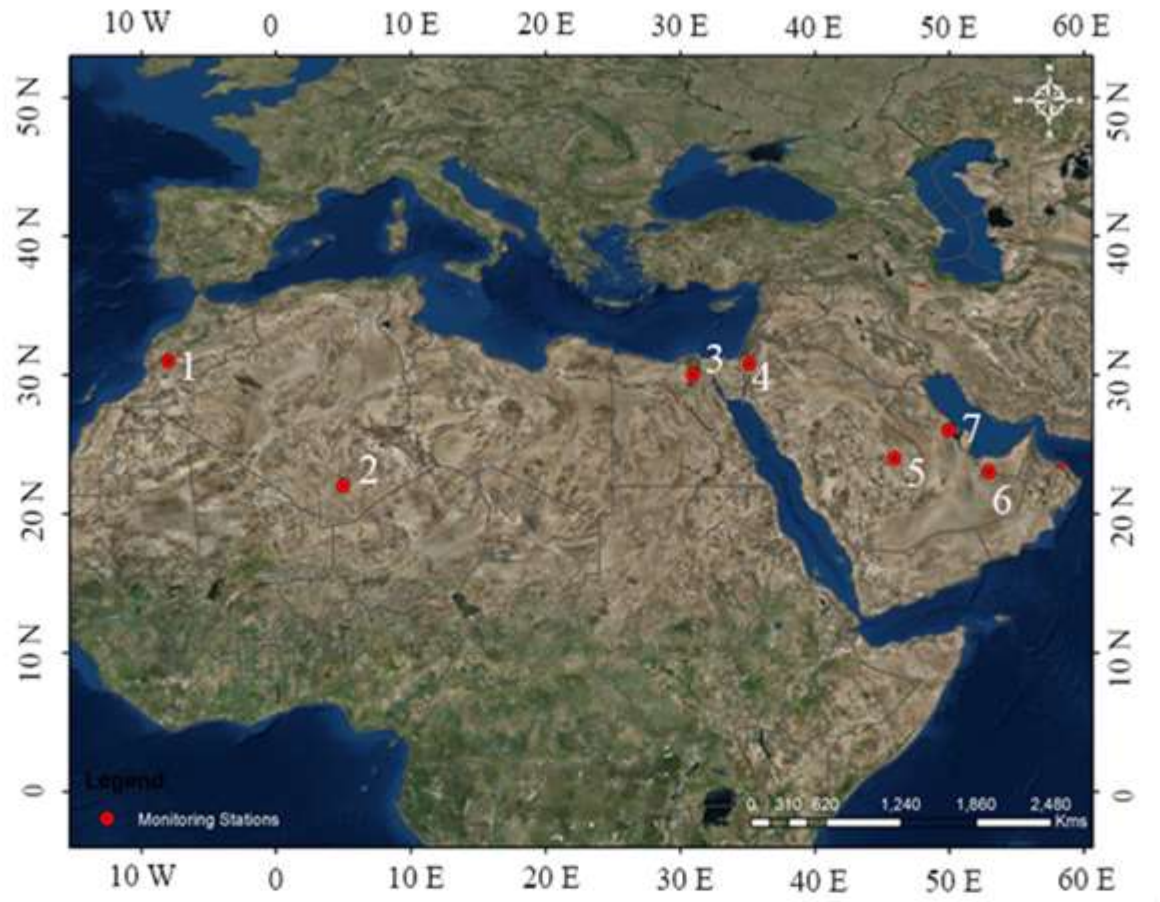
10 W
0
10 E
20 E
30 E
40 E
50 E
60 E
50 N
40 N
30 N
20 N
10 N
0
1
2
3
4
5
6
7
Legend
Monitoring Stations
0 310 620 1,240 1,860 2,480
Kms

Figure 1.

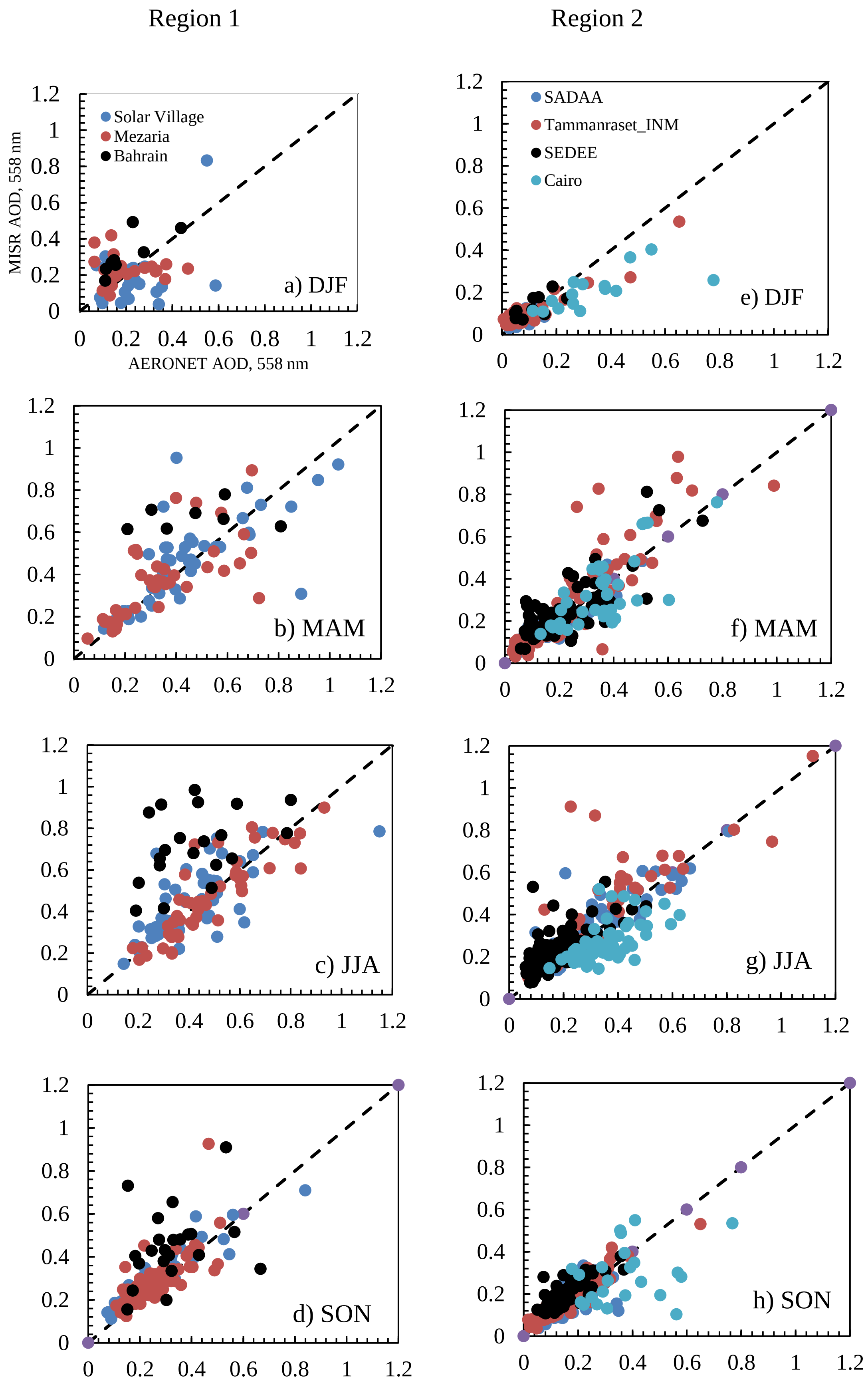
Region 1
Region 2
MISR AOD, 558 nm
AERONET AOD, 558 nm
Solar Village
Mezaria
Bahrain
SADAA
Tammanraset_INM
SEDEE
Cairo
a) DJF
b) MAM
c) JJA
d) SON
e) DJF
f) MAM
g) JJA
h) SON

Figure 2

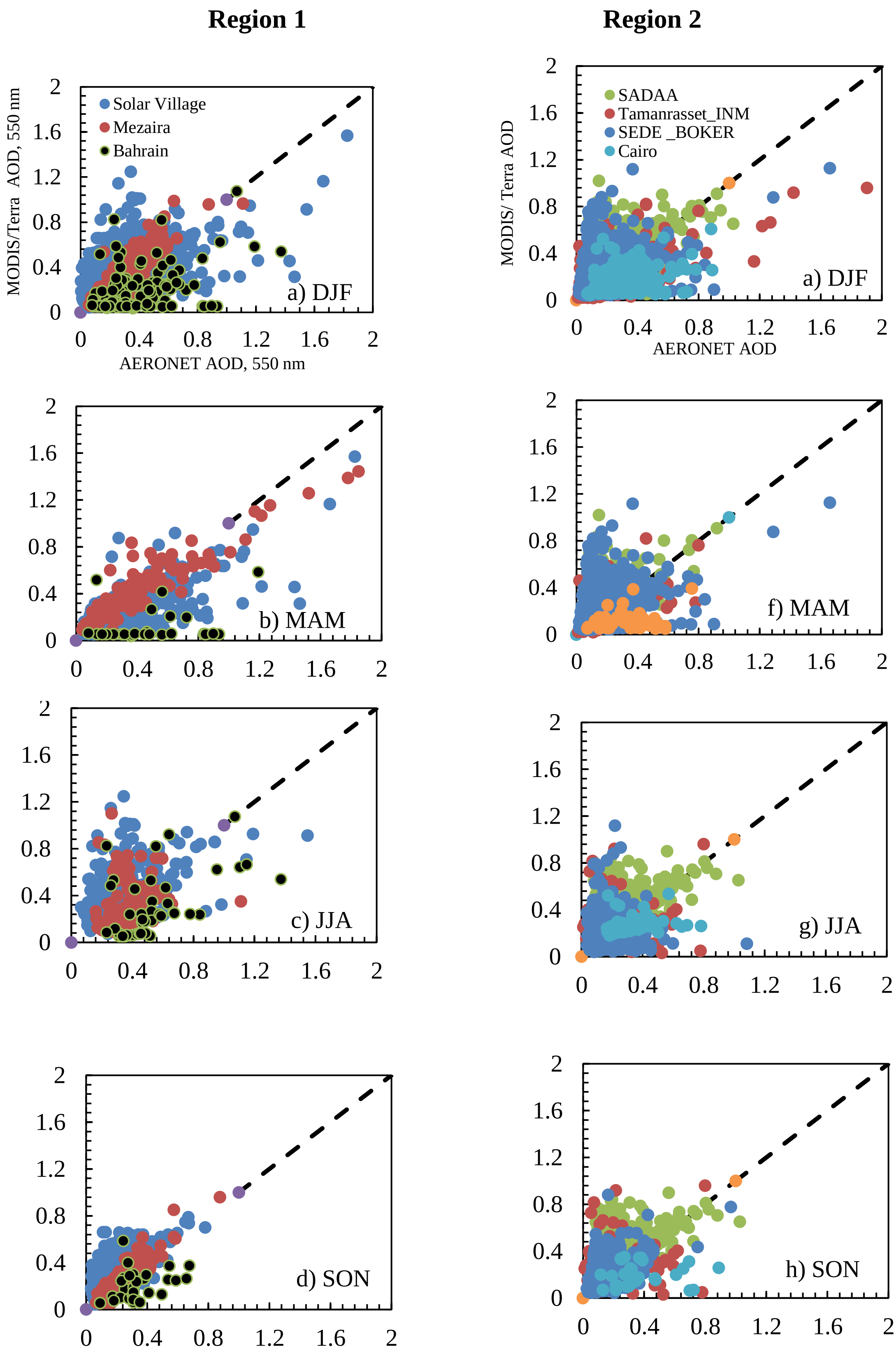
Region 1
Region 2
Solar Village
Mezaira
Bahrain
MODIS/Terra AOD, 550 nm
AERONET AOD, 550 nm
a) DJF
b) MAM
c) JJA
d) SON
SADAA
Tamanrasset_INM
SEDE _BOKER
Cairo
MODIS/ Terra AOD
AERONET AOD
a) DJF
f) MAM
g) JJA
h) SON

Figure 3.

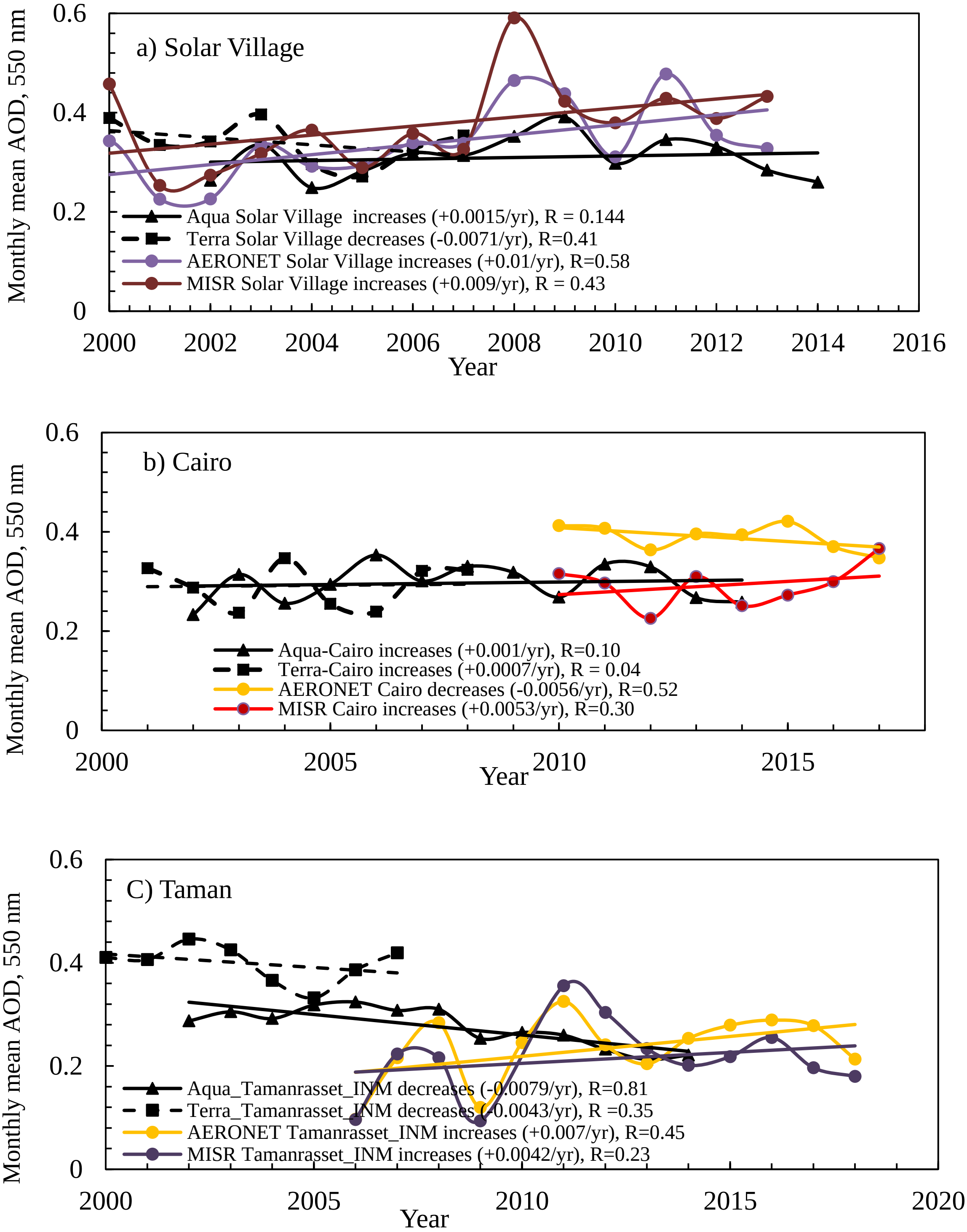
a) Solar Village
Monthly mean AOD, 550 nm
0.6
0.4
0.2
0
2000
2002
2004
2006
2008
2010
2012
2014
2016
Year
Aqua Solar Village increases (+0.0015/yr), R = 0.144
Terra Solar Village decreases (-0.0071/yr), R=0.41
AERONET Solar Village increases (+0.01/yr), R=0.58
MISR Solar Village increases (+0.009/yr), R = 0.43
b) Cairo
Monthly mean AOD, 550 nm
0.6
0.4
0.2
0
2000
2005
2010
2015
Year
Aqua-Cairo increases (+0.001/yr), R=0.10
Terra-Cairo increases (+0.0007/yr), R = 0.04
AERONET Cairo decreases (-0.0056/yr), R=0.52
MISR Cairo increases (+0.0053/yr), R=0.30
C) Taman
Monthly mean AOD, 550 nm
0.6
0.4
0.2
0
2000
2005
2010
2015
2020
Year
Aqua_Tamanrasset_INM decreases (-0.0079/yr), R=0.81
Terra_Tamanrasset_INM decreases (-0.0043/yr), R =0.35
AERONET Tamanrasset_INM increases (+0.007/yr), R=0.45
MISR Tamanrasset_INM increases (+0.0042/yr), R=0.23

Figure 4.

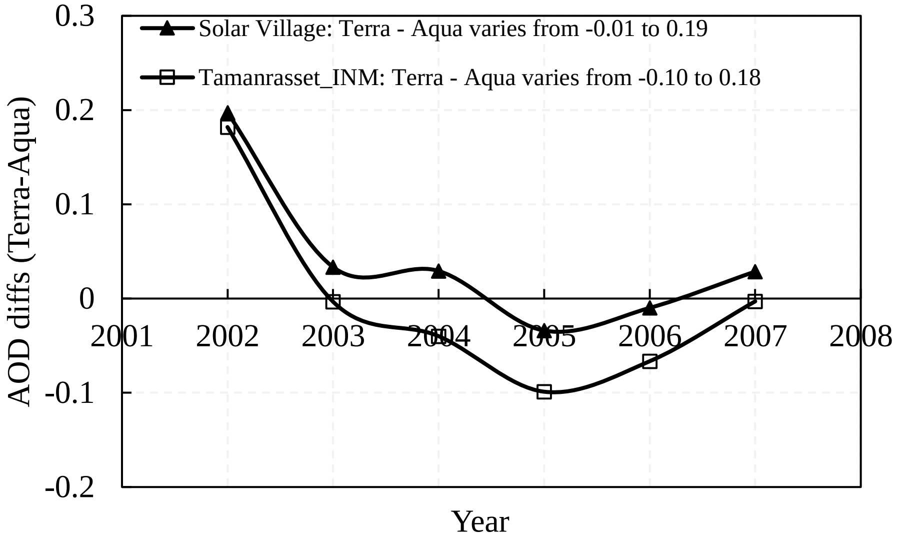
Solar Village: Terra - Aqua varies from -0.01 to 0.19
Tamanrasset_INM: Terra - Aqua varies from -0.10 to 0.18
AOD diffs (Terra-Aqua)
0.3
0.2
0.1
0
-0.1
-0.2
2001
2002
2003
2004
2005
2006
2007
2008
Year

Figure 5.

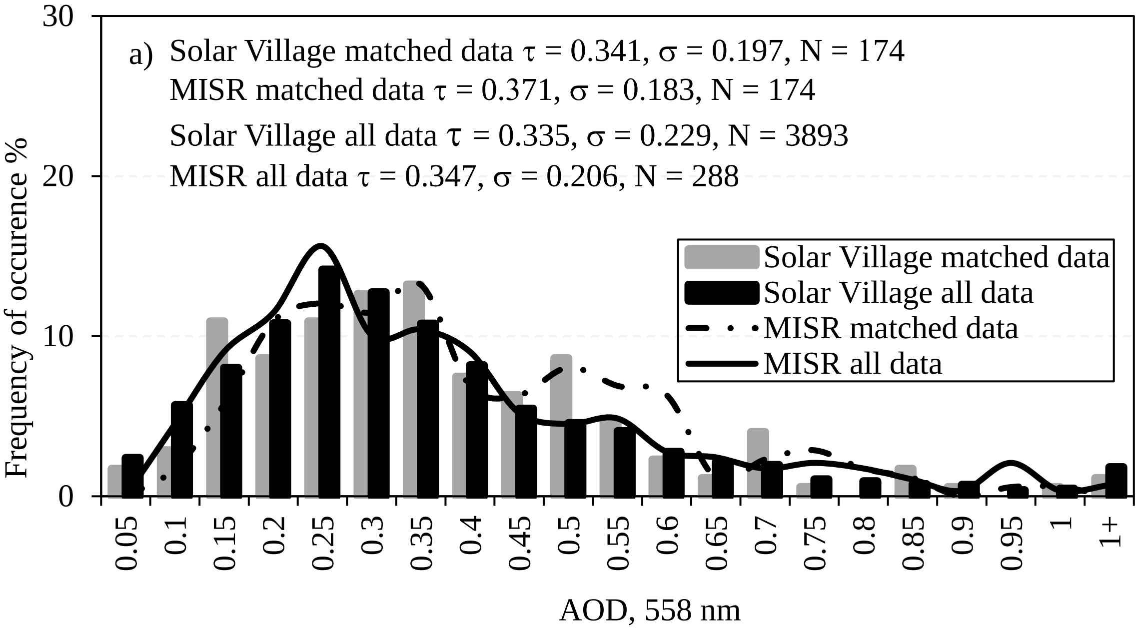

a) Solar Village matched data τ = 0.341, σ = 0.197, N = 174
MISR matched data τ = 0.371, σ = 0.183, N = 174
Solar Village all data τ = 0.335, σ = 0.229, N = 3893
MISR all data τ = 0.347, σ = 0.206, N = 288
Solar Village matched data
Solar Village all data
MISR matched data
MISR all data
Frequency of occurence %
0
10
20
30
0.05
0.1
0.15
0.2
0.25
0.3
0.35
0.4
0.45
0.5
0.55
0.6
0.65
0.7
0.75
0.8
0.85
0.9
0.95
1
1+
AOD, 558 nm

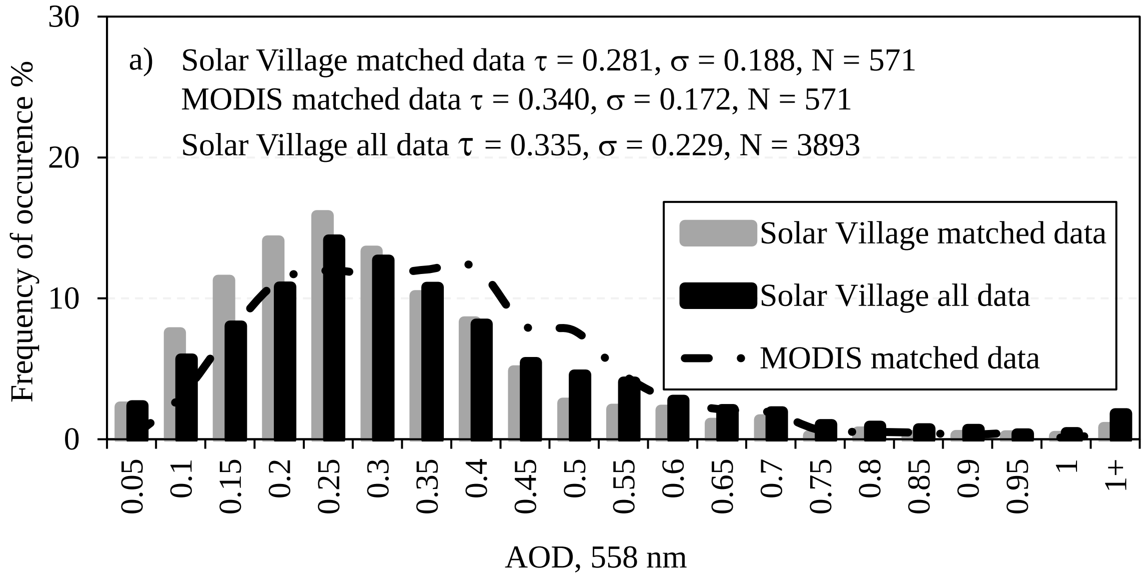

a) Solar Village matched data τ = 0.281, σ = 0.188, N = 571
MODIS matched data τ = 0.340, σ = 0.172, N = 571
Solar Village all data τ = 0.335, σ = 0.229, N = 3893
Solar Village matched data
Solar Village all data
MODIS matched data
Frequency of occurence %
0
10
20
30
0.05
0.1
0.15
0.2
0.25
0.3
0.35
0.4
0.45
0.5
0.55
0.6
0.65
0.7
0.75
0.8
0.85
0.9
0.95
1
1+
AOD, 558 nm

Figure 6.

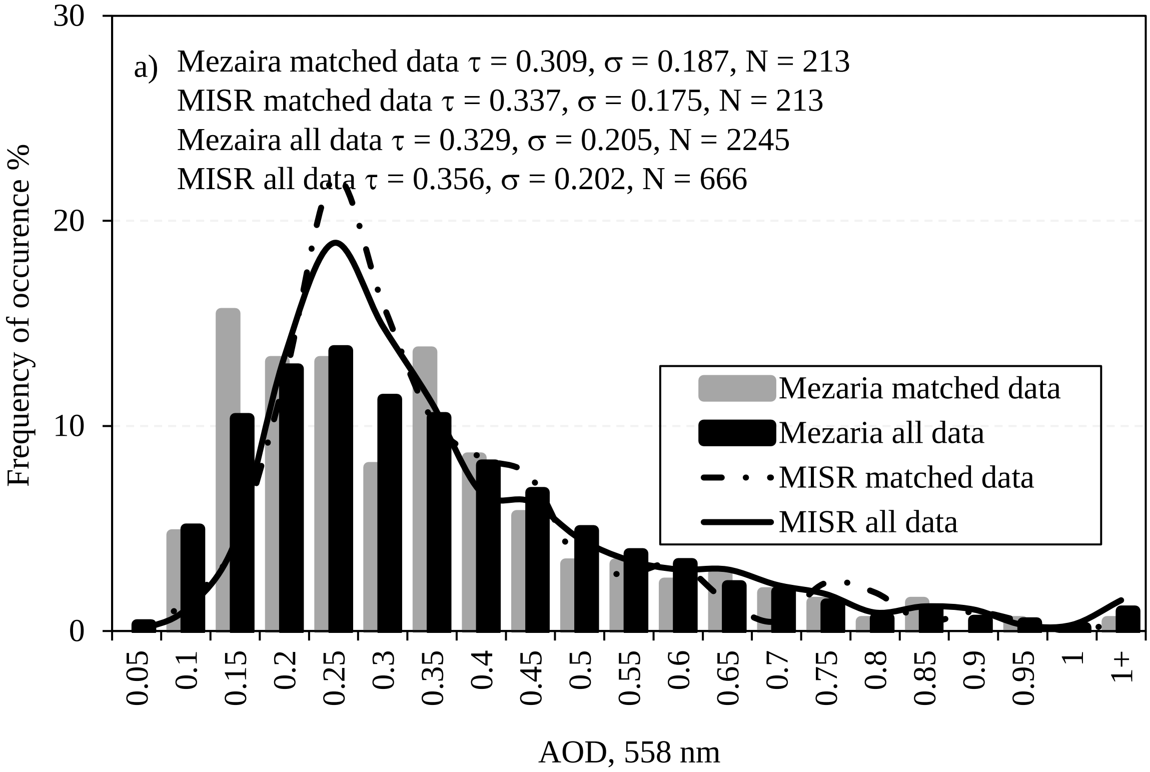
a) Mezaira matched data τ = 0.309, σ = 0.187, N = 213
MISR matched data τ = 0.337, σ = 0.175, N = 213
Mezaira all data τ = 0.329, σ = 0.205, N = 2245
MISR all data τ = 0.356, σ = 0.202, N = 666
Mezaria matched data
Mezaria all data
MISR matched data
MISR all data
Frequency of occurence %
AOD, 558 nm

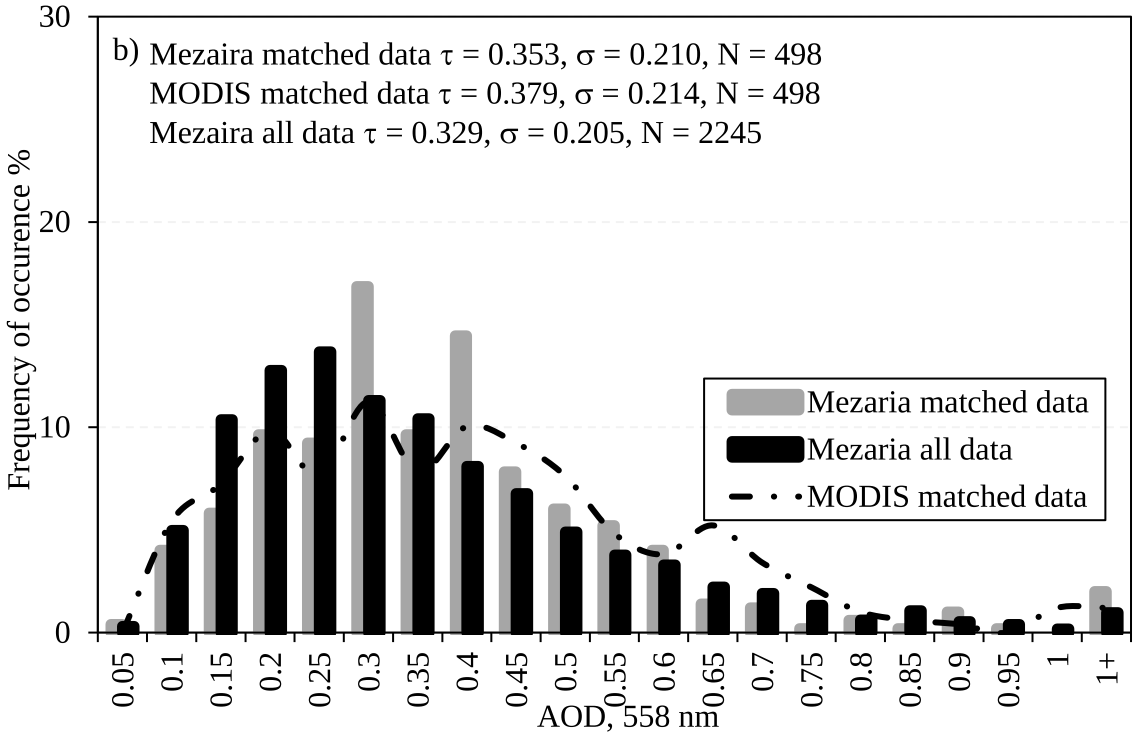
b) Mezaira matched data τ = 0.353, σ = 0.210, N = 498
MODIS matched data τ = 0.379, σ = 0.214, N = 498
Mezaira all data τ = 0.329, σ = 0.205, N = 2245
Mezaria matched data
Mezaria all data
MODIS matched data
Frequency of occurence %
AOD, 558 nm

982 Figure 7.

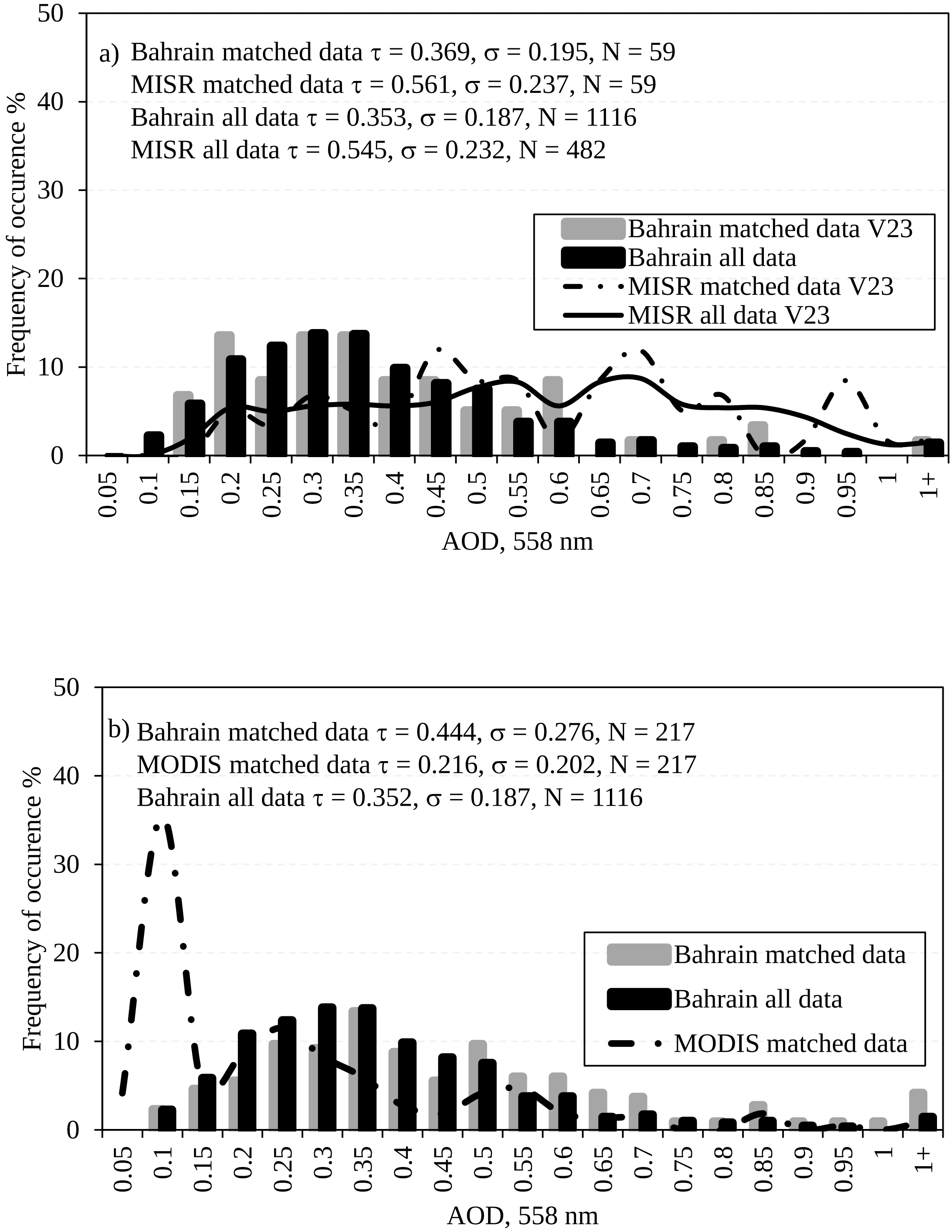
a) Bahrain matched data τ = 0.369, σ = 0.195, N = 59
MISR matched data τ = 0.561, σ = 0.237, N = 59
Bahrain all data τ = 0.353, σ = 0.187, N = 1116
MISR all data τ = 0.545, σ = 0.232, N = 482
Bahrain matched data V23
Bahrain all data
MISR matched data V23
MISR all data V23
Frequency of occurence %
0
10
20
30
40
50
0.05
0.1
0.15
0.2
0.25
0.3
0.35
0.4
0.45
0.5
0.55
0.6
0.65
0.7
0.75
0.8
0.85
0.9
0.95
1
1+
AOD, 558 nm
b) Bahrain matched data τ = 0.444, σ = 0.276, N = 217
MODIS matched data τ = 0.216, σ = 0.202, N = 217
Bahrain all data τ = 0.352, σ = 0.187, N = 1116
Bahrain matched data
Bahrain all data
MODIS matched data
Frequency of occurence %
0
10
20
30
40
50
0.05
0.1
0.15
0.2
0.25
0.3
0.35
0.4
0.45
0.5
0.55
0.6
0.65
0.7
0.75
0.8
0.85
0.9
0.95
1
1+
AOD, 558 nm

Figure 8.

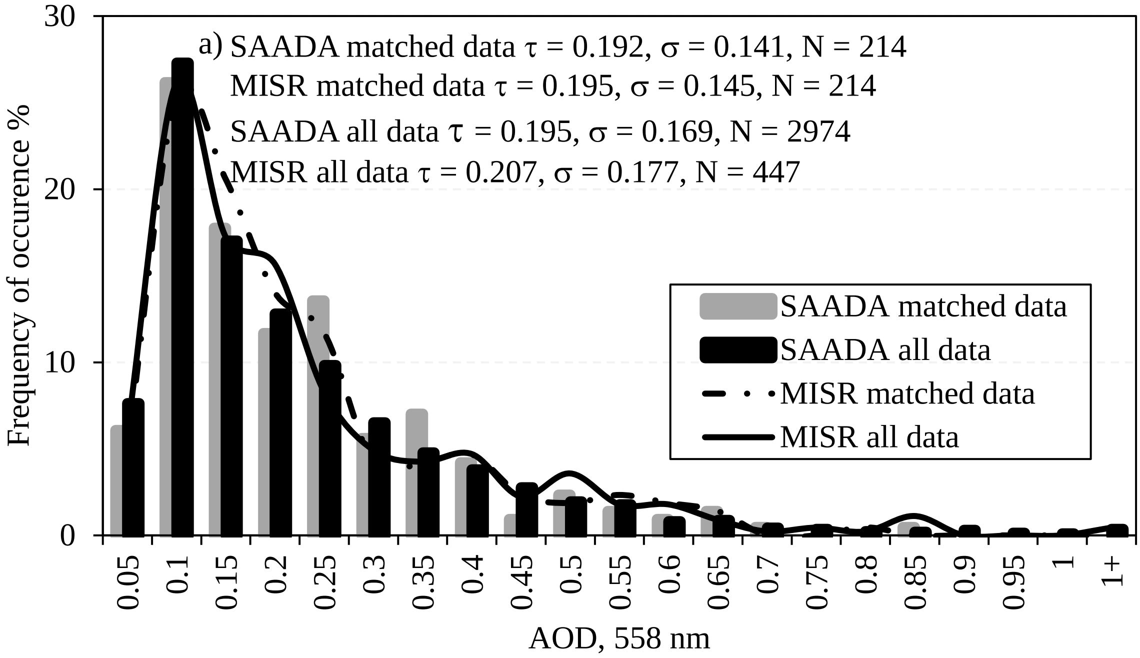
a) SAADA matched data τ = 0.192, σ = 0.141, N = 214
MISR matched data τ = 0.195, σ = 0.145, N = 214
SAADA all data τ = 0.195, σ = 0.169, N = 2974
MISR all data τ = 0.207, σ = 0.177, N = 447
SAADA matched data
SAADA all data
MISR matched data
MISR all data
Frequency of occurence %
0
10
20
30
0.05
0.1
0.15
0.2
0.25
0.3
0.35
0.4
0.45
0.5
0.55
0.6
0.65
0.7
0.75
0.8
0.85
0.9
0.95
1
1+
AOD, 558 nm

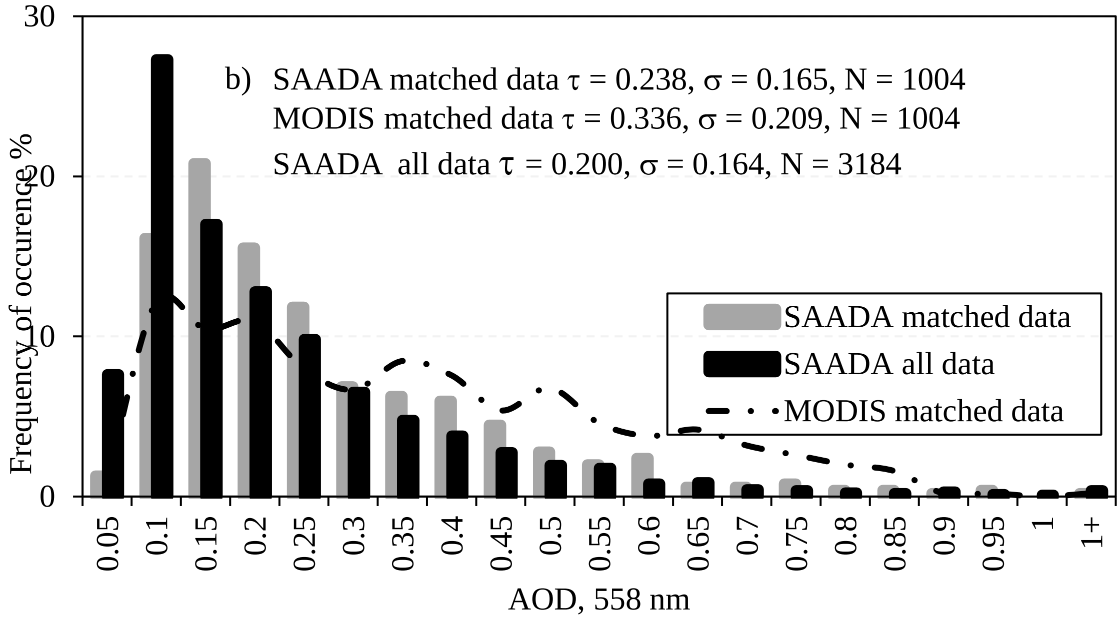
b) SAADA matched data τ = 0.238, σ = 0.165, N = 1004
MODIS matched data τ = 0.336, σ = 0.209, N = 1004
SAADA all data τ = 0.200, σ = 0.164, N = 3184
SAADA matched data
SAADA all data
MODIS matched data
Frequency of occurence %
0
10
20
30
0.05
0.1
0.15
0.2
0.25
0.3
0.35
0.4
0.45
0.5
0.55
0.6
0.65
0.7
0.75
0.8
0.85
0.9
0.95
1
1+
AOD, 558 nm

Figure 9.

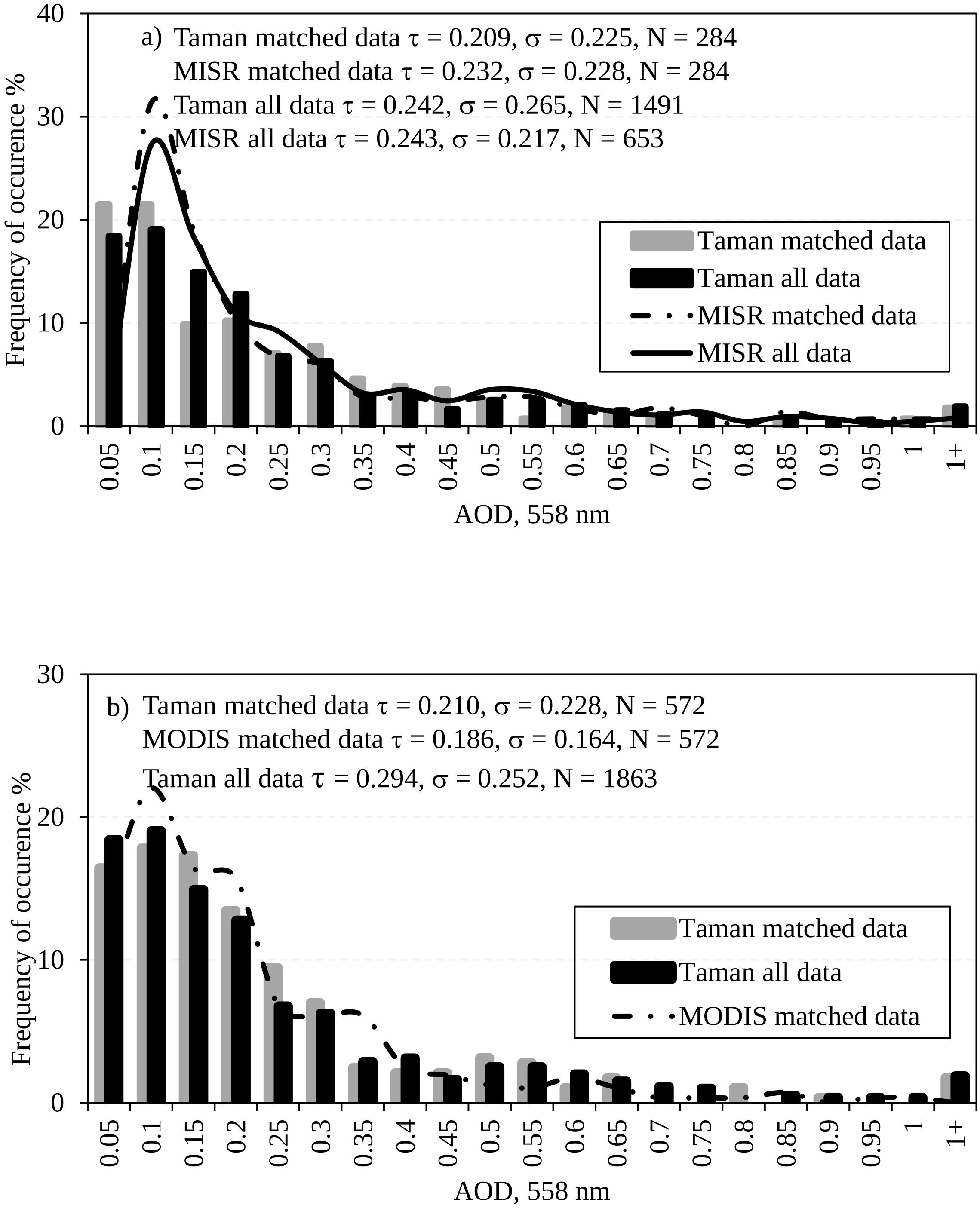

a) Taman matched data τ = 0.209, σ = 0.225, N = 284
MISR matched data τ = 0.232, σ = 0.228, N = 284
Taman all data τ = 0.242, σ = 0.265, N = 1491
MISR all data τ = 0.243, σ = 0.217, N = 653
Taman matched data
Taman all data
MISR matched data
MISR all data
Frequency of occurence %
0
10
20
30
40
0.05
0.1
0.15
0.2
0.25
0.3
0.35
0.4
0.45
0.5
0.55
0.6
0.65
0.7
0.75
0.8
0.85
0.9
0.95
1
1+
AOD, 558 nm
b) Taman matched data τ = 0.210, σ = 0.228, N = 572
MODIS matched data τ = 0.186, σ = 0.164, N = 572
Taman all data τ = 0.294, σ = 0.252, N = 1863
Taman matched data
Taman all data
MODIS matched data
Frequency of occurence %
0
10
20
30
0.05
0.1
0.15
0.2
0.25
0.3
0.35
0.4
0.45
0.5
0.55
0.6
0.65
0.7
0.75
0.8
0.85
0.9
0.95
1
1+
AOD, 558 nm

Figure 10.

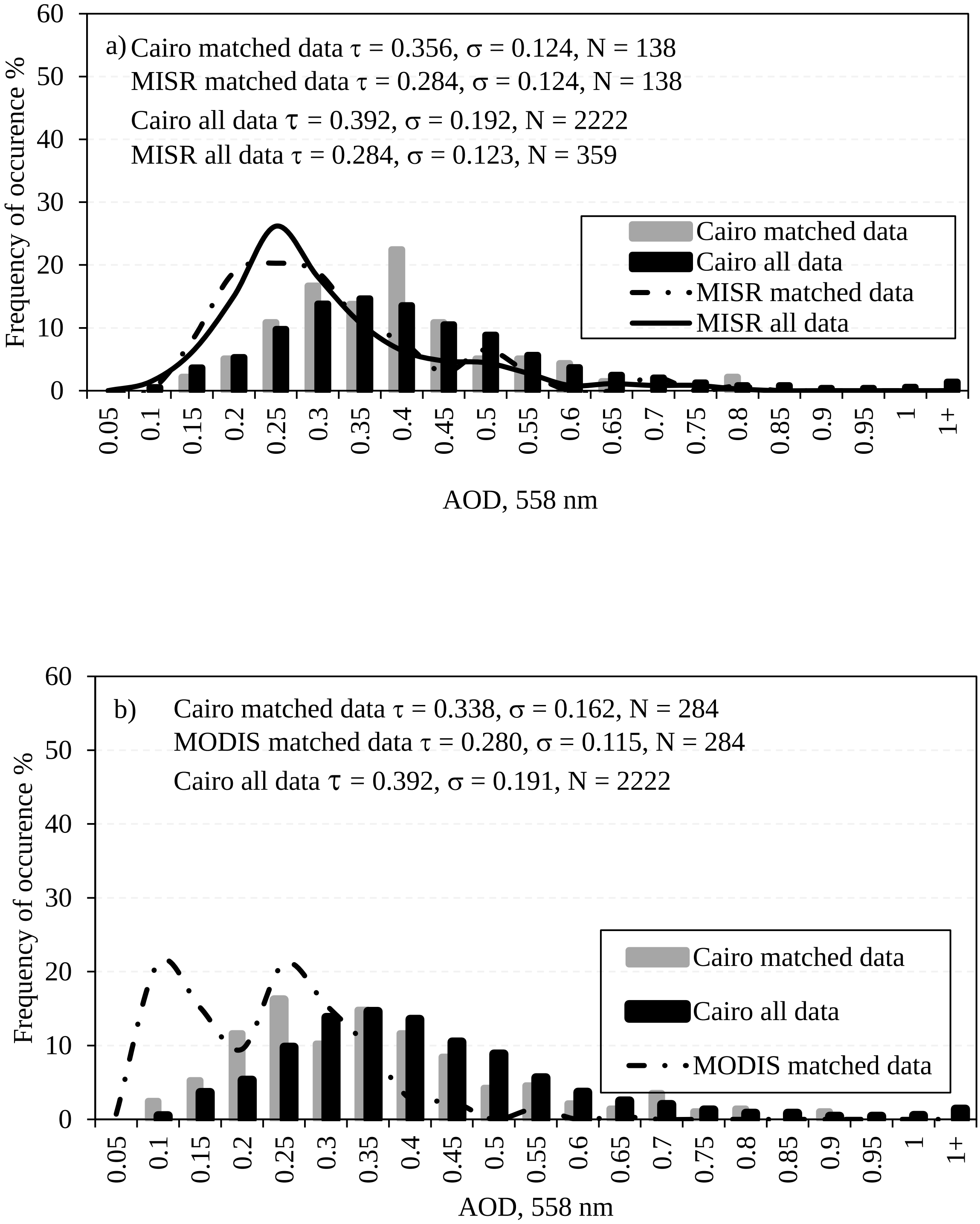
a) Cairo matched data τ = 0.356, σ = 0.124, N = 138
MISR matched data τ = 0.284, σ = 0.124, N = 138
Cairo all data τ = 0.392, σ = 0.192, N = 2222
MISR all data τ = 0.284, σ = 0.123, N = 359
Cairo matched data
Cairo all data
MISR matched data
MISR all data
Frequency of occurence %
0
10
20
30
40
50
60
0.05
0.1
0.15
0.2
0.25
0.3
0.35
0.4
0.45
0.5
0.55
0.6
0.65
0.7
0.75
0.8
0.85
0.9
0.95
1
1+
AOD, 558 nm
b) Cairo matched data τ = 0.338, σ = 0.162, N = 284
MODIS matched data τ = 0.280, σ = 0.115, N = 284
Cairo all data τ = 0.392, σ = 0.191, N = 2222
Cairo matched data
Cairo all data
MODIS matched data
Frequency of occurence %
AOD, 558 nm

Figure 11.

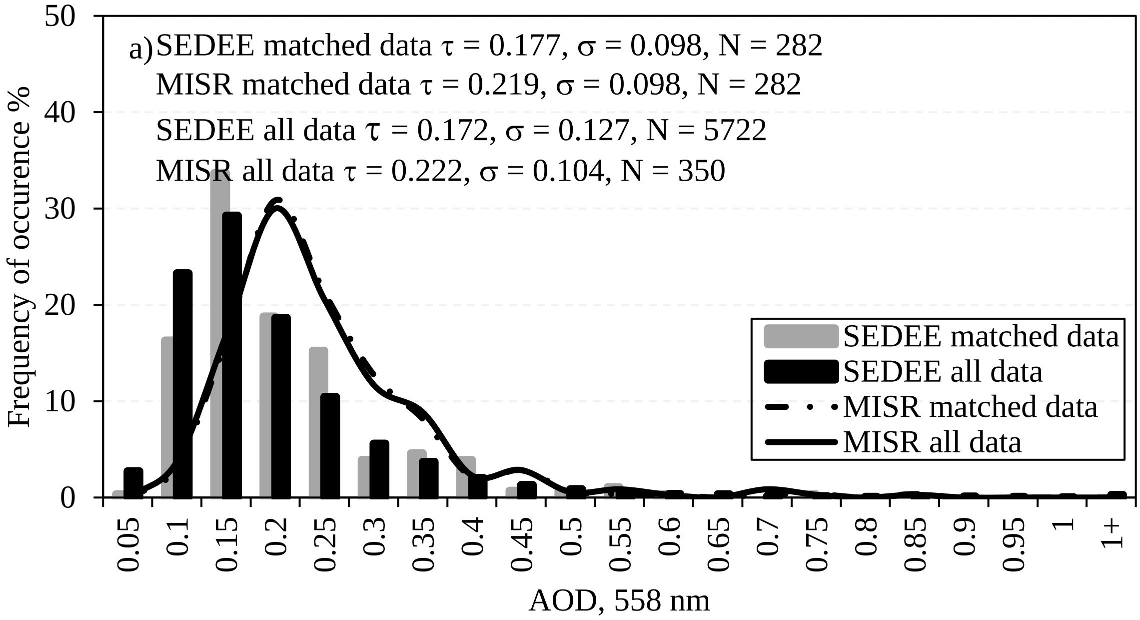
a)
SEDEE matched data τ = 0.177, σ = 0.098, N = 282
MISR matched data τ = 0.219, σ = 0.098, N = 282
SEDEE all data τ = 0.172, σ = 0.127, N = 5722
MISR all data τ = 0.222, σ = 0.104, N = 350
SEDEE matched data
SEDEE all data
MISR matched data
MISR all data
Frequency of occurence %
AOD, 558 nm
0
10
20
30
40
50
0.05
0.1
0.15
0.2
0.25
0.3
0.35
0.4
0.45
0.5
0.55
0.6
0.65
0.7
0.75
0.8
0.85
0.9
0.95
1
1+

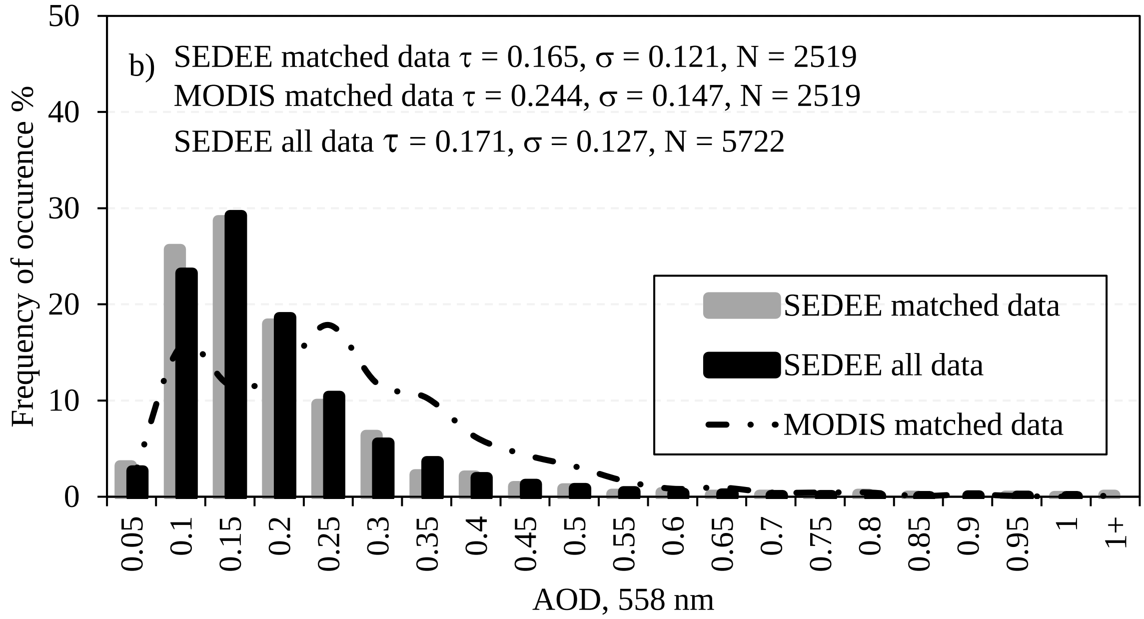
b)
SEDEE matched data τ = 0.165, σ = 0.121, N = 2519
MODIS matched data τ = 0.244, σ = 0.147, N = 2519
SEDEE all data τ = 0.171, σ = 0.127, N = 5722
SEDEE matched data
SEDEE all data
MODIS matched data
Frequency of occurence %
AOD, 558 nm
0
10
20
30
40
50
0.05
0.1
0.15
0.2
0.25
0.3
0.35
0.4
0.45
0.5
0.55
0.6
0.65
0.7
0.75
0.8
0.85
0.9
0.95
1
1+

Figure 12.